MISCELLANEOUS REPORT NO. 3

MISSISSIPPIAN PALEOSOLS, PALEOKARST, AND EOLIAN CARBONATES IN INDIANA

by

Donald E. Hattin and J. Robert Dodd

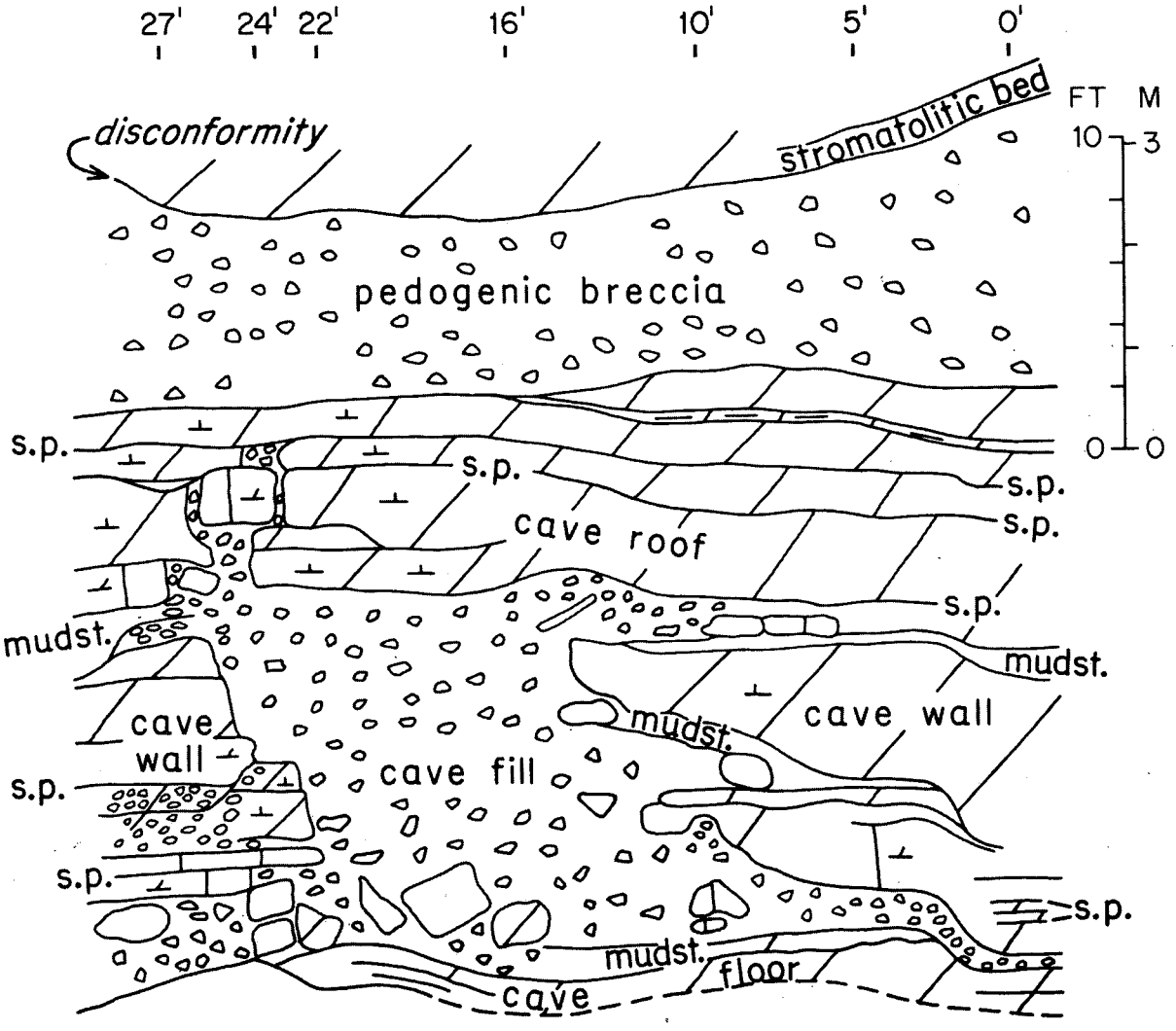

prepared for the 1992 Annual Meeting
of the Geological Society of America

DIVISION OF GEOLOGICAL SURVEY
4383 FOUNTAIN SQUARE DRIVE
COLUMBUS, OHIO 43224-1362
(614) 265-6576 (Voice)
(614) 265-6994 (TDD)
(614) 447-1918 (FAX)

OHIO GEOLOGY ADVISORY COUNCIL

SCIENTIFIC AND TECHNICAL STAFF OF THE DIVISION OF GEOLOGICAL SURVEY

ADMINISTRATION (614) 265-6576

Thomas M. Berg, MS, *State Geologist and Division Chief*
Robert G. Van Horn, MS, *Assistant State Geologist and Assistant Division Chief*
Michael C. Hansen, PhD, *Senior Geologist,* Ohio Geology *Editor, and Geohazards Officer*
James M. Miller, BA, *Fiscal Officer*
Sharon L. Stone, AD, *Executive Secretary*

REGIONAL GEOLOGY SECTION (614) 265-6597

Dennis N. Hull, MS, *Geologist Manager and Section Head*

Paleozoic Geology and Mapping Subsection (614) 265-6473
Edward Mac Swinford, MS, *Geologist Supervisor*
Glenn E. Larsen, MS, *Geologist*
Gregory A. Schumacher, MS, *Geologist*
Douglas L. Shrake, MS, *Geologist*
Ernie R. Slucher, MS, *Geologist*

Quaternary Geology and Mapping Subsection (614) 265-6599
Richard R. Pavey, MS, *Geologist Supervisor*
C. Scott Brockman, MS, *Geologist*

Core Drilling Subsection (614) 265-6594
Douglas L. Crowell, MS, *Geologist Supervisor*
Roy T. Dawson, *Driller*
Michael J. Mitchell, *Driller*
Mark E. Clary, *Drilling Assistant*
William R. Dunfee, *Drilling Assistant*

SUBSURFACE STRATIGRAPHY AND PETROLEUM GEOLOGY SECTION (614) 265-6585

Ronald G. Rea, MS, *Geologist Supervisor and Section Head*
Mark T. Baranoski, MS, *Geologist*
James McDonald, MS, *Geologist*
Ronald A. Riley, MS, *Geologist*
Lawrence H. Wickstrom, MS, *Senior Geologist and Computer Coordinator*
Angelena M. Bailey, *Administrative Assistant*

Samples and Records
Garry E. Yates, NZCS, *Environmental Technology Supervisor*

TECHNICAL PUBLICATIONS SECTION (614) 265-6593

Merrianne Hackathorn, MS, *Geologist and Editor*
Jean M. Lesher, *Typesetting and Printing Technician*
Edward V. Kuehnle, BA, *Cartographer*
Michael R. Lester, BS, *Cartographer*
Robert L. Stewart, *Cartographer*
Lisa Van Doren, BA, *Cartographer*

PUBLICATIONS CENTER (614) 265-6605

Garry E. Yates, NZCS, *Public Information Officer and Acting Section Head*
Inaleigh E. Eisen, *Public Inquiries Assistant*
Donna M. Schrappe, *Public Inquiries Assistant*
Billie Long, *Account Clerk*

MINERAL RESOURCES AND GEOCHEMISTRY SECTION (614) 265-6602

David A. Stith, MS, *Geologist Supervisor and Section Head*
Allan G. Axon, PhD, *Geologist*
Richard W. Carlton, PhD, *Senior Geologist*
Norman F. Knapp, PhD, *Chemical Laboratory Supervisor*
Sherry L. Weisgarber, MS, *Geologist and Mineral Statistician*
Kim E. Vorbau, BS, *Geologist*

LAKE ERIE GEOLOGY SECTION (419) 626-4296

Scudder D. Mackey, PhD, *Geologist Supervisor and Section Head*
Danielle A. Foye, BS, *Geology Technician*
Jonathan A. Fuller, MS, *Geologist*
Donald E. Guy, Jr., MS, *Geologist*
Dale L. Liebenthal, *Operations Officer & Research Vessel Operator*
Mary Lou McGurk, *Office Assistant*

STATE OF OHIO
George V. Voinovich, Governor
DEPARTMENT OF NATURAL RESOURCES
Frances S. Buchholzer, Director
DIVISION OF GEOLOGICAL SURVEY
Thomas M. Berg, Chief

MISCELLANEOUS REPORT NO. 3

MISSISSIPPIAN PALEOSOLS, PALEOKARST, AND EOLIAN CARBONATES IN INDIANA

by

Donald E. Hattin and J. Robert Dodd
Department of Geological Sciences
Indiana University

Field Trip 13 for the Annual Meeting
of the Geological Society of America
Cincinnati, Ohio
October 26-29, 1992

sponsored by the Sedimentary Geology Division
of the Geological Society of America

Columbus
1992

Typesetting and layout: Graphic Directions
Cartographic assistance: Robert L. Stewart and
Edward V. Kuehnle

Cover illustration: Diagram of St. Louis Limestone in cliff face at Stop 6 showing large body of breccia filling Valmeyeran paleocavern. See figure 30.

CONTENTS

FIGURES

CONTENTS

TABLE

MISSISSIPPIAN PALEOSOLS, PALEOKARST, AND EOLIAN CARBONATES IN INDIANA

by
Donald E. Hattin
and
J. Robert Dodd

INTRODUCTION

The St. Louis and Ste. Genevieve Limestones were deposited on a broad, shallow-water marine platform that extended across a large part of the present-day upper Mississippi Valley region during Mississippian time, approximately 325 million years ago (fig. 1). These formations contain a number of subaerial exposure features such as soil horizons, solution features, and wind-blown deposits, suggesting that sea level fell repeatedly, exposing the area to subaerial weathering, erosion, and deposition. Principal field-trip objectives include examination of evidence that suggests emergence of Valmeyeran platform-carbonate sediments, discussion of mechanisms by which such emergence could have occurred, and discussion of possible relationship of such emergences to global sea-level fluctuations. To these ends, participants will study texture, structure, and composition of the St. Louis and Ste. Genevieve Limestones in man-made and natural exposures on the Mitchell Plain, which is a karstic region developed on middle Mississippian carbonate rocks of southern Indiana. Much of what participants will see has been discovered within the past three years, and except in abstract form many of the data and conclusions have not been published previously.

Within the Ste. Genevieve, which will be visited first, the emergence surfaces are associated in part with mixed-clast carbonate grainstones that include texture, composition, and sedimentary structures that collectively denote origin in coastal eolian environments. These eolianites will then be compared with a lenticular body of oolitic grainstone that was deposited under high-energy shoal-water marine conditions. A third Ste. Genevieve exposure manifests a classical regressive section that terminates in supratidal rocks that have been altered by pedogenic processes.

Emergence surfaces in the St. Louis Limestone occur in parts of the section that contain such features as laminated micrites, stromatolites, mud cracks, intraclastic rocks, birdseye structure, alveolar structure, brecciated rock, and evidence of evaporites. These features suggest shallow subtidal to supratidal deposition under conditions of marine hypersalinity.

The last stop will enable participants to evaluate a spectacular example of buried paleokarst that includes caverns, pedogenic breccias, sinkholes, remnants of terra rossa and gley soils, and evidence of cavern collapse during Valmeyeran time.

CHRONOSTRATIGRAPHIC UNITS		LITHOSTRATIGRAPHIC UNITS	
SYSTEM	SERIES	GROUP	FORMATION
MISSISSIPPIAN	CHESTERIAN	BUFFALO WALLOW	(13 FORMATIONS)
		STEPHENSPORT	
		WEST BADEN	
	VALMEYERAN	BLUE RIVER	PAOLI LS.
			STE. GENEVIEVE LS.
			ST. LOUIS LS.
		SANDERS	SALEM LS. HARRODSBURG LS. RAMP CREEK FM.
		BORDEN	EDWARDSVILLE FM.
			SPICKERT KNOB FM.
			NEW PROVIDENCE SHALE
	KINDERHOOKIAN		ROCKFORD LS.
			NEW ALBANY SH.

FIGURE 1.—Classification of Mississippian strata in Indiana, highlighting positions of the St. Louis and Ste. Genevieve Limestones.

PHYSIOGRAPHY

Most of the field-trip route (fig. 2) lies within the Interior Low Plateaus physiographic province, and all of the geologic stops are situated therein. During the return trip to Cincinnati, we will cross the boundary that separates nonglaciated from glaciated terrains, and the final part of the trip will thence traverse a part of the Central Lowlands physiographic province.

From Cincinnati to Louisville (fig. 2) the route lies within the Outer Bluegrass section of the Interior Low Plateaus. This section is developed on gently westward-dipping strata that range in age from Late Ordovician to Late Devonian and are dominated by carbonate rocks and shale. Most of the region is characterized by an upland surface that is in the late-youth stage of dissection. Upland summits are remarkably accordant, lying between 900 and 1,000 feet (275-300 m) above sea level, and manifest a well-preserved Tertiary erosion surface known as the Lexington-Highland Rim Peneplain (Thornbury, 1965). In the Cincinnati area, summit elevations range from 800 to 900 feet (245-275 m) descending westward to 550 to 600 feet (170-185 m) just east of Louisville.

The westernmost part of the Outer Bluegrass section is a lowland developed on late Devonian-earliest Mississippian organic-rich rock known as New Albany Shale. At Louisville, we shall cross the Ohio River into Indiana and, after brief transit of the black-shale belt (in Indiana called the Scottsburg Lowland by Malott, 1922), ascend the face slope of a major cuesta (Knobstone Escarpment) that is held up by deltaic marine siltstones of the Borden Group (Valmeyeran). This escarpment has local relief of 623 feet (190 m) near the Ohio River in Floyd County, Indiana (west of Louisville), and marks the eastern edge of an immaturely dissected, heavily forested plateau known as the Norman Upland (Malott, 1922). As in the Outer Bluegrass section, the dip is gently westward away from the Cincinnati Arch at approximately 25 to 30 feet per mile (5 to 6 m per km). Along the Day 1 field-trip route the upland is approximately 8 miles (13 km) wide and slopes westward from 900 feet (275 m) at the eastern edge to approximately 800 feet (245 m) in the west.

Middle and Upper Valmeyeran carbonate strata that lie above the Borden siltstones underlie the rolling karstic surface of the Mitchell Plain (Beede, 1911). Throughout this section of the Interior Low Plateaus the land surface is dimpled by thousands of sinkholes and is underlain by extensive cavern systems that for generations have lured speleologists, spelunkers, and tourists to the region. The Mitchell Plain physiographic section is better suited to agricultural pursuits than is the Norman Upland, and the landscape is correspondingly more grassland than forest. Caverns and canyons developed in Valmeyeran carbonate rocks are featured attractions of Spring Mill State Park, which is the site of our overnight stop, and McCormick's Creek State Park, which is the site of our last stop on Day 2. The Mitchell Plain is widest and the karst topography best developed between Paoli and Spring Mill State Park, in the area that we shall cross late in the afternoon of Day 1 (fig. 2).

Surface elevations on the Mitchell Plain range from 650 to 900 feet (200-275 m) in the field-trip area, and the plain is underlain by as much as 450 feet (135 m) of middle Mississippian carbonate rocks. Throughout the district, long-term humid-climate weathering has produced cherty terra rossa soils that can be seen at the top of several road cuts on State Road 37 between Bedford and Bloomington (Day 2). Within the Mitchell Plain, limestone is quarried extensively for use as a construction material, and a shoal-water grainstone facies of the Salem Limestone (fig. 1) is quarried on a large scale for use as building stone throughout the United States.

Along its western edge the Mitchell Plain gives way to steeply ascending wooded slopes of the Chester Escarpment, which is held up by late Mississippian rocks of the Chesterian Series and delineates the eastern margin of the hilly and wooded Crawford Upland (Malott, 1922). On Day 1 we shall traverse the eastern portion of this upland while proceeding northwestward on U.S. Highway 150, and on Day 2 we shall cross a small outlier of the upland just east of our last stop, McCormick's Creek State Park.

During the return trip to Cincinnati on Day 2, the route recrosses the Mitchell Plain and the Norman Upland on State Road 46. Between Nashville and Columbus, Indiana, the highway crosses the boundary between the Interior Low Plateaus province and the Central Lowlands province, which in this region was glaciated. Just west of Columbus, the route descends the Knobstone Escarpment and enters a division of the Central Lowlands known as the Scottsburg Lowland, which contains scattered tracts of vegetated Pleistocene sand dunes. East of Columbus, relatively level farmlands of the Scottsburg Lowland give way to undulating landscapes of the Muscatatuck Regional Slope. This physiographic district is a structurally controlled surface developed on Silurian and Devonian carbonate rocks.

At Greensburg, Indiana, the field-trip route leaves State Road 46 to follow I-74 to Cincinnati. A few miles after turning onto I-74 the route enters a plateau area developed on Upper Ordovician rocks and called the Dearborn Upland. Surface elevations of this plateau, which is part of the Lexington-Highland Rim Peneplain, rise to more than 1,100 feet (335 m) above sea level. Collectively, the Scottsburg Lowland, Muscatatuck Regional Slope, and Dearborn Upland are Indiana equivalents of the Outer Bluegrass section, where we started and shall end this excursion.

STE. GENEVIEVE LIMESTONE

The Ste. Genevieve Limestone is geographically widespread, occurring throughout the Illinois Basin. Indeed, rocks of probably correlative age and similar lithology occur over much of the eastern part of the North American craton. As presently defined, the Ste. Genevieve conformably overlies the St. Louis Limestone and is in turn conformably overlain by the Paoli Limestone (fig. 1). The unit contains a number of lithofacies, including ooid grainstone, skeletal grainstone, mixed-clast grainstone, mudstone, and wackestone. Lithologic components include ooids, skeletal fragments, peloids, dolomite, chert, and minor amounts of siliciclastic sand and silt. Most carbonate lithologies were probably deposited in shallow marine settings, either on high-energy shoals or in lagoons. Some units of the Ste. Genevieve consist of marine-derived carbonate grains that have been reworked by eolian processes (Hunter 1988, 1989). Some intervals also show extensive effects of subaerial exposure such as pedogenic brecciation, calcrete, and

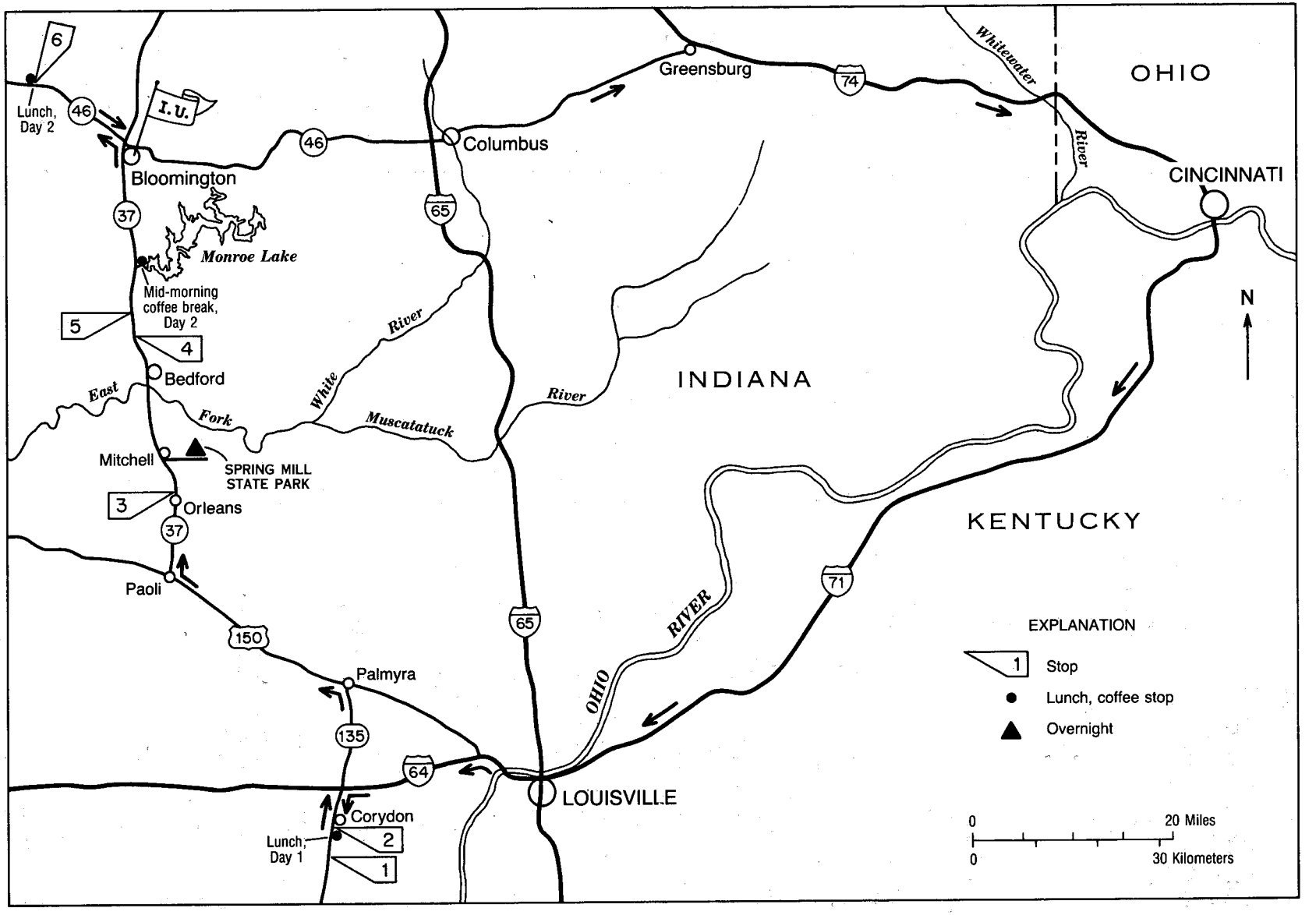

FIGURE 2.—Map of field-trip route.

rhizomorphs (Leibold, 1982; Hunter, 1989; and Merkley, 1991).

Much of the earlier work on the Ste. Genevieve Limestone was of a stratigraphic nature. The stratigraphy has recently been revised and reviewed by Droste and Carpenter (1990). Although the Ste. Genevieve Limestone is economically important, researchers have published relatively few studies of its depositional history. The most extensive study, based mainly on outcrop sections, was that of Carr (1973). He emphasized the origin of ooid shoals and concluded that they had many characteristics in common with modern Bahamian ooid shoals and probably had a similar origin. He made many measurements of cross-bedding direction and concluded that orientation of the shoals was primarily controlled by tidal currents. Dodd and others (1990a) have recently continued the study of an ooid shoal at Orleans and concluded that the shoal migrated into the area, probably on a hardground surface, primarily as a result of rapid deposition during storms. Knewtson and Hubert (1969) conducted a detailed study of cross-bedding directions and diagenetic features of the Ste. Genevieve Limestone in Missouri. Choquette and Steinen (1980) made an important contribution to understanding of depositional patterns in Ste. Genevieve ooid shoals and associated facies in subsurface samples from the Illinois Basin. Cluff and Lineback (1981) and Cluff (1984) have also interpreted ooid grainstones in the subsurface of Illinois and Indiana as forming on shoals of limited geographic extent. They interpret muddier facies as deposits of intershoal areas. A number of students at Indiana University have written M.S. theses on shoal-related petroleum fields in the Illinois Basin (*e.g.*, Zinn, 1983; Perrin, 1986; and Ray, 1986).

One of the main objects of this trip is to examine the eolian facies and associated exposure surfaces in the Ste. Genevieve Limestone in the Corydon area. Hunter (1988, 1989) was first to identify eolianites at the two exposures we will be examining on State Road 135 south of Corydon and in other sections of the Corydon area. He has also tentatively identified carbonate eolianites at the type locality in Ste. Genevieve, Missouri. Merkley (1991) has traced the eolianite units across the Ohio River into Kentucky as far south as Irvington. Our preliminary work suggests that eolian deposits occur at least as far south in Kentucky as Upton and perhaps almost to Bowling Green. Hanford (1990) has recently reinterpreted a subsurface section of Ste. Genevieve-equivalent rock in southwestern Kansas as containing eolian grainstone. Although Pleistocene and Holocene carbonate eolianites are common, descriptions of pre-Pleistocene carbonate eolian deposits are rare. To the best of our knowledge, the only other well-documented examples are from Pennsylvanian and Permian carbonate rocks in the Grand Canyon area (Loope, 1986; Rice and Loope, 1987, 1991; Loope and Haverland, 1988).

Hunter originally identified the eolian deposits largely on the basis of such sedimentologic features as varvelike laminations produced by climbing wind ripples, inverse grading of some of these laminae, rarity of ripple foreset laminae in climbing-ripple stratification, low height/length ratio of ripples, lack of grains larger than 4 mm, and exposure surfaces above and below eolian units. Hunter (1989) has described these features in detail in an earlier guidebook.

We have found distinctive petrographic differences between eolian and marine grainstones in the Corydon stratigraphic sections (table 1). In most cases, differences between eolian and marine grainstones are readily explainable in terms of their different origins. Quartz, particularly sand-sized grains, is common in eolian samples (fig. 3). Quartz grains are more readily transported across land than through a mosaic of shoals and intershoal areas at sea. Broken ooids also are common in eolian samples (fig. 4). They are more readily fractured by impact during saltation on land than in marine environments. Winds blowing across a variety of exposed carbonate environments yield the high grain diversity of eolian grainstones (fig. 5). Marine shoals tend to be dominated by formation of a particular type of grain (fig. 6). Experimental data and observation show that rounding and production of spherical grains is characteristic of eolian samples (fig. 5). Well-lithified intraclasts (fig. 7) are produced by subaerial cementation that is more complete than cementation in the marine environment. Fine laminations, good sorting, and inverse grading (fig. 8) are all products of climbing-ripple stratification produced in eolian environments (Hunter, 1989). Lack of large grains in eolian grainstone is a result of the inability of wind to carry large particles. Solution packing in eolian grainstones (figs. 3-5) is more difficult to explain. Apparently little cement formed in these rocks at shallow depths, perhaps because the dry climate limited the amount of water in the vadose zone. Lack of cement between grains allowed extensive packing of the grains during burial. Formation of marine cement in the marine grainstones prevented extensive solution packing. Vadose cements and loose packing might be expected in carbonate eolianites deposited in more humid climates.

TABLE 1.—*Comparison of petrographic properties of eolian and marine grainstones in the Ste. Genevieve Limestone at Corydon (from Dodd and others, in press).*

Property	Eolian	Marine
Detrital quartz	present	absent
Broken ooids	present	absent
Grain diversity	high	low
Rounding & sphericity	high sphericity	rounded, not spherical
Intraclasts	well lithified	poorly lithified
Laminations	present	absent
Sorting	good within laminae, poor between	generally good
Inverse grading	present	absent
Large grains	absent	may be present
Solution packing	extensive	minor

The Ste. Genevieve Limestone contains a number of features suggesting multiple periods of exposure above sea level. Hunter (1989) and Merkley (1991) have described as many as four separate units of eolianite separated by marine deposits. These eolianites thus indicate at least local periods of exposure. The widespread Bryantsville Breccia (seen at Stop 4) has been used to define the top of the Ste. Genevieve Limestone in outcrop. Leibold (1982) has interpreted the Bryantsville Breccia Bed as a paleosol that was formed during subaerial exposure of the unit. Similar breccias (fig. 9) occur lower in the formation as well (Hunter, 1989; Dodd and others, 1990b; Merkley, 1991) suggesting other periods of exposure. Dodd and others (1990a) recognized a hardground surface that was lithified before deposition of an ooid shoal at Orleans, Indiana (Stop 3). They suggested that lithification may have occurred during subaerial exposure. Hunter (1989) and Merkley (1991) also identified rhizomorphs (fig. 10) and calcrete development in association with the eolian units. At least six exposure surfaces, including the surface above the Bryantsville Breccia, at the top of the formation, have been described from the

FIGURE 3.—Abundant quartz silt (white, angular grains) in eolian grainstone. Note close packing and high sphericity of grains. Scale bar = 0.5 mm.

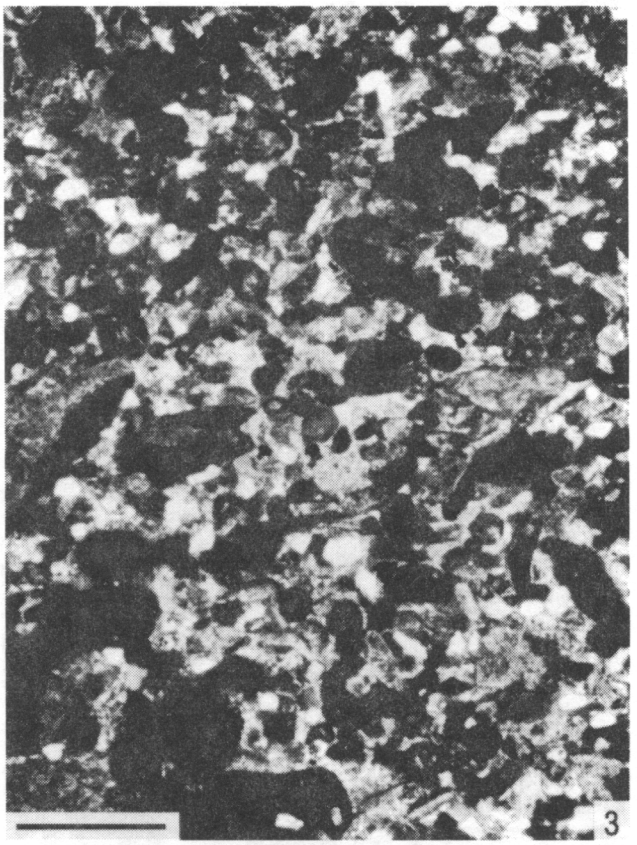

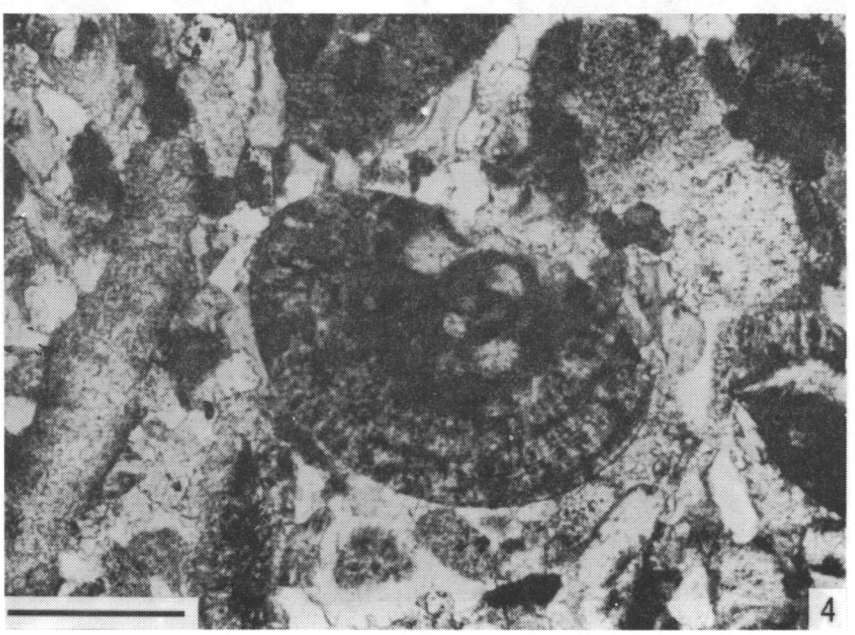

FIGURE 4.—Broken, abraded ooid and solution at grain contacts in eolian grainstone. Scale bar = 0.25 mm.

FIGURE 5.—Very well rounded grains with high sphericity in eolian grainstone. Note rounding of intraclast, close packing of grains, and high grain diversity. Scale bar = 0.5 mm.

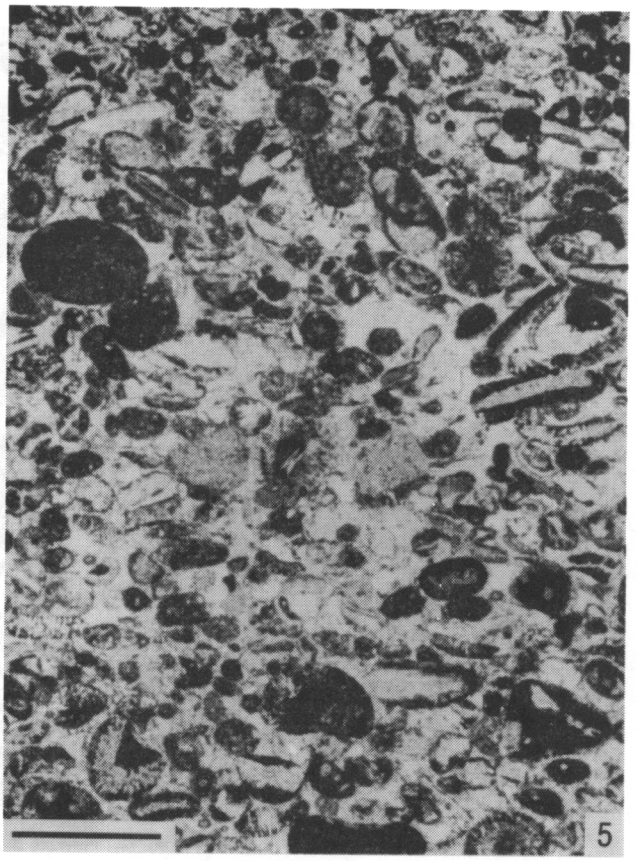

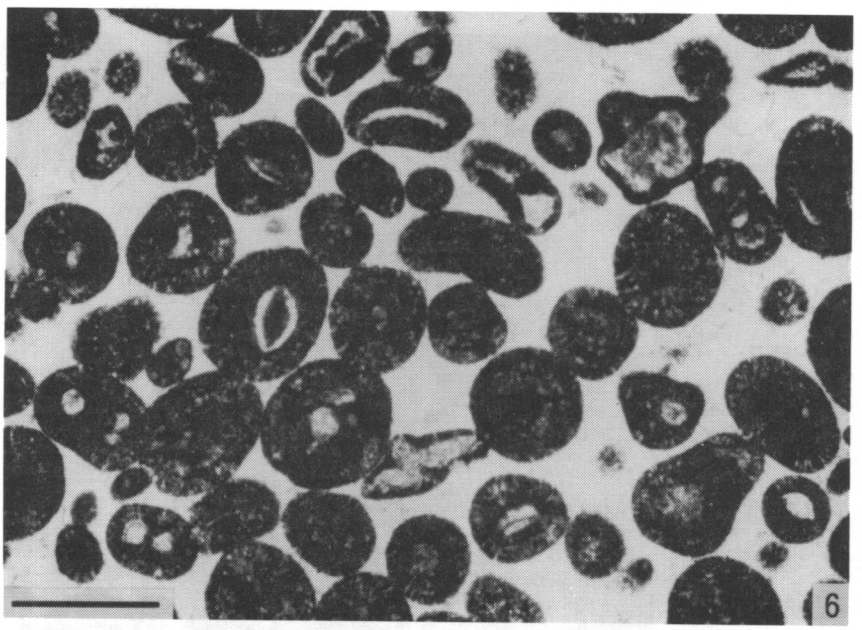

FIGURE 6.—Sample composed almost entirely of ooids or grains with oolitic coatings in marine grainstone. Note loose packing of grains. Scale bar = 0.5 mm.

FIGURE 7.—Spherical intraclast in eolian grainstone showing equal abrasion across constituent grains and cement. Scale bar = 0.5 mm.

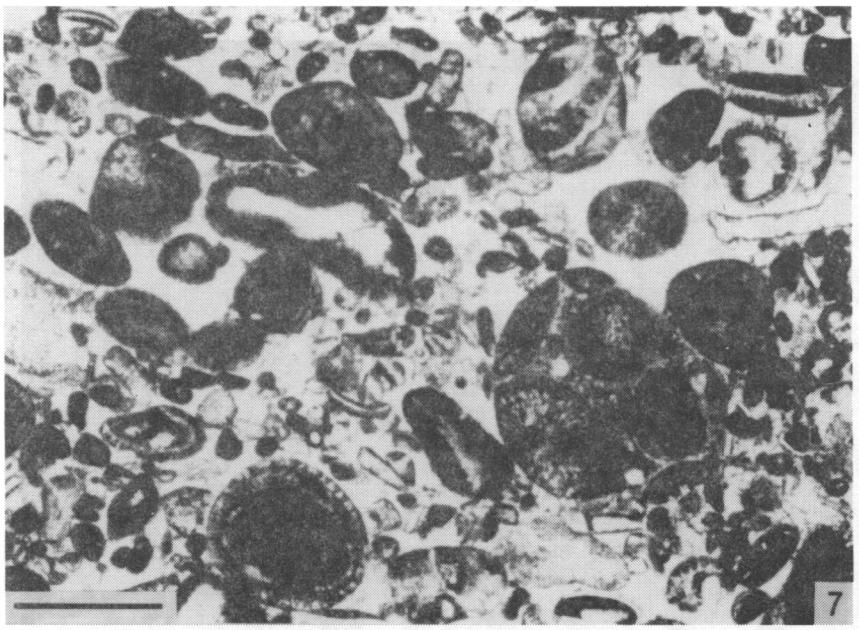

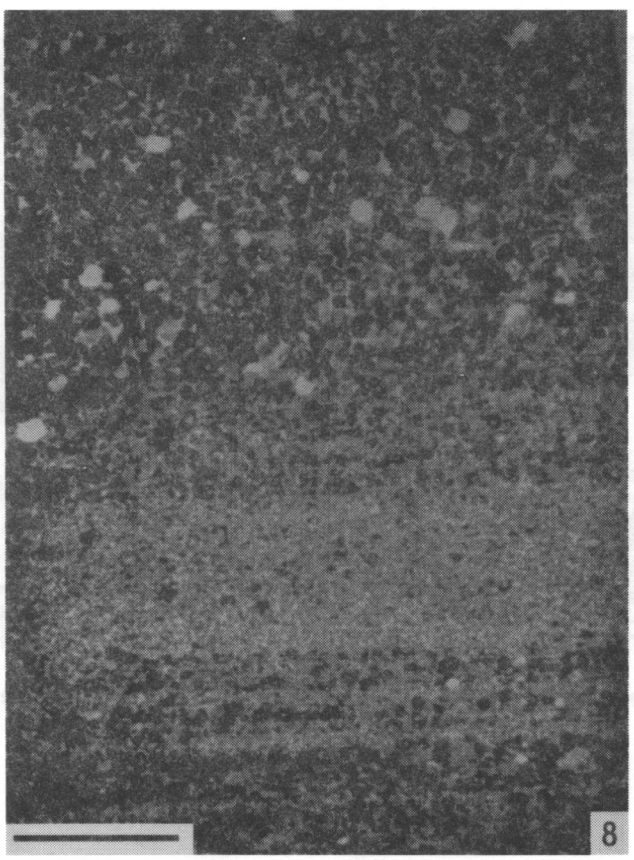

FIGURE 8.—Laminated eolian grainstone. Note reverse grading in thick upper lamination. White grains are quartz. Scale bar = 4 mm.

FIGURE 9.—Brecciation of sample below exposure surface. Note calcrete around clasts. Scale bar = 0.5 mm.

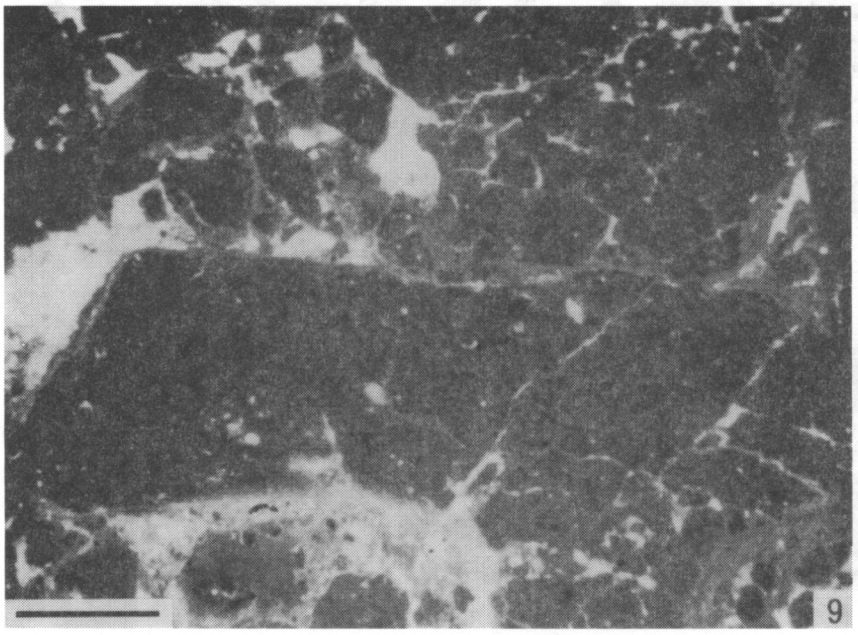

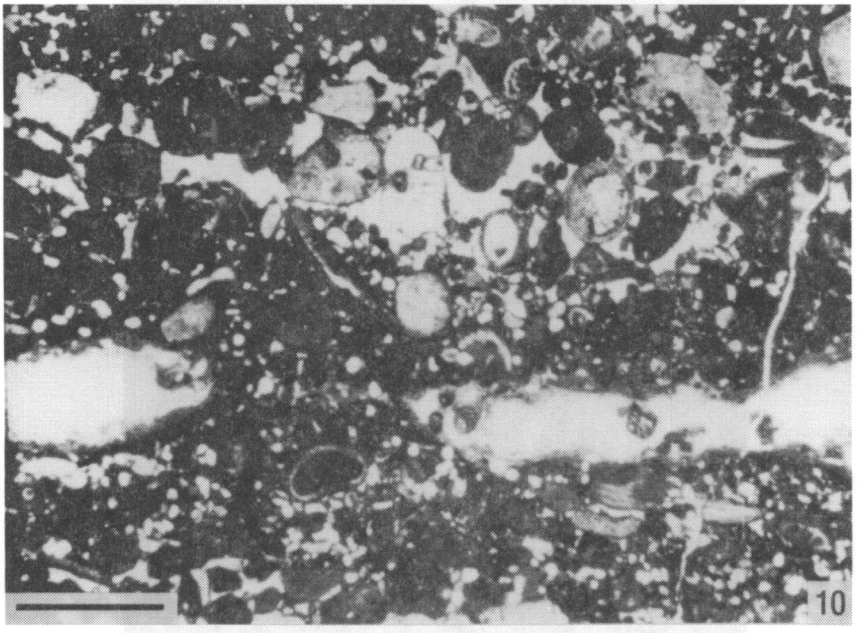

FIGURE 10.—Rhizoliths coated with calcrete in sample taken from beneath exposure surface. Scale bar = 0.5 mm.

Ste. Genevieve. These surfaces have been tentatively correlated in the Corydon region (Merkley, 1991). In addition to these features related to soil formation, mud cracks and stromatolites suggest extremely shallow water and at least brief exposure.

Two models of origin have been suggested for formation of eolianites in the Ste. Genevieve Limestone: (1) Marine waves, currents, and tides may have built shoals above sea level. Once exposed, the shoals would have been subject to eolian processes, which would expand the islands both vertically and laterally. This process is common in formation of barrier islands as well as offshore islands today. (2) Sea level may have fallen, exposing broad areas of carbonate sediment. Sea-level variation may have resulted either from worldwide eustatic fluctuation or from more local tectonism. Winds blowing across these areas would produce dunes and eolian deposits.

Deposits produced by these two models should have a number of differences. Eolian deposits resulting from the island model would likely be of limited geographic extent and probably could not be correlated over large distances. Eolian deposits should commonly rest on high-energy shoal deposits without an intervening exposure surface. Eolian deposits forming on islands should consist largely of grains derived from the underlying shoal and thus would be no more diverse than that shoal. Siliciclastic sand and to a lesser extent silt should not be common in eolian deposits associated with islands. Sand grains would be difficult to transport from a mainland source to an offshore shoal which might be separated from land by an intervening low-energy lagoon or intershoal area.

Eolianites produced by a general lowering of sea level would be more extensive and should be correlatable over a larger area. They would normally be expected to overlie exposure surfaces formed when sea level fell. They could overlie any marine facies, as they need not be directly associated with high-energy shoal deposits. Grain type should be diverse because winds could mix grains from a variety of now-exposed marine environments. Siliciclastic sand and silt could be easily transported overland by winds from the source area. The features listed in this paragraph are characteristics of the Ste. Genevieve eolianites, indicating that they formed after a fall in sea level. As pointed out by Rice and Loope (1991), the sea-level variation that led to production of the eolianites may be related to the beginning of continental ice formation that climaxed in Late Paleozoic time.

A consequence of the sea-level-fall model is that the eolian deposits overlie an unconformity and thus mark the base of a stratigraphic sequence. Five sequences have tentatively been identified in the St. Genevieve Limestone. They can be correlated along the outcrop for at least 30 miles (50 km) and probably extend much farther. In concept, if they result from basinwide lowering of sea level, they should be traceable throughout the Illinois Basin. Application of sequence-stratigraphic methods will allow more detailed correlation than was previously possible in this formation and can be used to more precisely define the depositional history of the Ste. Genevieve.

ST. LOUIS LIMESTONE

DEFINITION

Problems regarding definition of the Salem-St.Louis and St. Louis-Ste. Genevieve contacts in outcrop and in the subsurface are summarized by Shaver and others (1986), Brown (1990), and Droste and Carpenter (1990). Differing sets of criteria are used by various authors, and some important discontinuities are not mentioned at all, suggesting the need for embracive stratigraphic and sedimentologic analysis of the St. Louis and adjacent strata throughout southwestern Indiana. In the Day 2 field-trip area, the Salem-St. Louis contact is defined by a prominent bed of grayish-green silty illitic shale that is 0.18 foot (5 cm) thick at Stop 5 but nearby is as much as 1.73 feet (0.53 m) thick. In the Indiana outcrop, thickness of the Salem ranges from 60 to 100 feet (18 to 20 m) (Shaver and others, 1986). Near its top, the Salem Limestone comprises a generally fining upward sequence dominated by skeletal grainstones that grade upward into packstones and wackestones (Brown, 1990; Brown and others, 1990). The grainstones are mostly deposits of shoals, intershoals, tidal channels, and sand flats, whereas the packstones and wackestones are products of deposition in quiet-water open or restricted lagoons and low-energy tidal channels. At Stop 5, the uppermost part of the Salem is a thick tabular bed of skeletal-pelletal packstone. This lithology contrasts markedly with the Salem section 10 miles (16 km) to the north, where the uppermost beds of the formation manifest large-scale channel-fill geometry and in part display well-preserved tidal lamination.

As defined by Shaver and others (1986), the base of the Ste. Genevieve lies approximately 20 feet (6 m) below a widespread marker known as the Lost River Chert Bed (Malott, 1952). However, Woodson (1982) includes the Lost River Chert in the Horse Cave Member of the St. Louis Limestone and selects as the St. Louis-Ste. Genevieve contact the base of the first bed of well-sorted, cross-bedded oolitic limestone above the chert bed. Rexroad and others (1990) note that the contact selected by Woodson corresponds to a widespread sharp break in conodont biostratigraphy, and they use both lithologic and paleontologic criteria to define the St. Louis-Ste. Genevieve contact in the Indiana outcrop. Overall, Ste. Genevieve rocks of the Indiana outcrop evince higher energy depositional environments than the St. Louis, contain an abundance of oolitic limestone, and tend to be lighter colored. The St. Louis Limestone is defined primarily by its bounding units, and comprises a nonhomogeneous sequence of mostly fine- to very fine-grained limestones, dolomitic limestones, and calcitic dolostones that are commonly separated by thin shale beds and locally contain deposits of gypsum.

CHARACTERISTICS

According to Jorgensen and Carr (1973), the St. Louis of Indiana and Kentucky can be divided informally into two units; the lower unit "consists mainly of silty dolomite, fine-grained limestone, anhydrite and gypsum," and the upper unit "consists mainly of fine-grained skeletal, pellet, and micritic limestones containing dense nodular chert." In studies of the southwestern Indiana subsurface, Keller and Becker (1980) and Droste and Carpenter (1990) also recognize two divisions of the St. Louis that are separated by a characteristic electric-log signature, the so-called X marker horizon. The lower unit, which Keller and Becker (1980) called the Sisson Member, comprises a sequence of "lighter colored grainstones and packstones that are interbedded with darker wackestones and mudstones typical of the lower St. Louis throughout the subsurface of Indiana" (Droste and Carpenter, 1990). According to Cluff (1984), the Sisson correlates with the upper part of the Salem Limestone of Illinois. Droste and Carpenter (1990) state, "The rocks of the upper and lower St. Louis are similar, but they also differ. Beds of gypsum and anhydrite are much less abundant in the upper rocks, oolitic and biofragmental rocks are distinctly more common in the upper rocks, and lighter colored rocks are somewhat more prominent in the upper rocks." Droste and Carpenter (1990) include the Lost River Chert in the Ste. Genevieve Limestone.

In general, the St. Louis Limestone of the Indiana outcrop is thinner bedded than the Ste. Genevieve and contains little oolitic limestone, much bedded and nodular chert in the upper part, and considerable dolomitic limestone and calcitic dolostone. The St. Louis includes numerous very thin beds or partings of dark-brownish-gray to greenish-gray silty shale and contains relatively few sparry-calcite-cemented grainstones. From the foregoing discussion, the conclusion may be drawn that the St. Louis is a very complex stratigraphic unit that has no simple description and is defined differently in the subsurface versus outcrop of southwestern Indiana.

In a core taken from south-central Greene County, Indiana, Jorgensen and Carr (1973) recognize pronounced cyclicity in the evaporite-bearing part of the St. Louis Limestone. Amongst 18 evaporite cycles recognized, they determined that a typical cycle comprises, from base to top, sediments deposited in intertidal, subtidal open lagoon, intertidal, and supratidal sabkha or restricted lagoon. In a detailed petrographic study of a St. Louis core taken in southwestern Monroe County, Indiana, Bagby (1989) recognizes eight microfacies. Six are carbonates that are interpreted as deposits of normal-marine shelf, open lagoon, restricted lagoon, intertidal/supratidal environments. The seventh facies, gypsum, is of evaporitic sabkha origin, and the eighth is a terrigenous clay-rich facies of probable eolian origin. Surface exposures of the St. Louis comprise a wide range of lithotypes, including both limestones and dolostones; grainstones, packstones, wackestones, and mudstones; rocks having skeletal, pelletal and intraclastic grain dominance; rocks containing cryptalgal, burrow, desiccation, birdseye, and cross-laminated structures; buried paleokarst; chert; and shales, including gray, brown, and black varieties. Apparent depositional environments range from open-marine shelf to supratidal.

In the field-trip area the St. Louis section is interrupted by at least three disconformities. One disconformity is marked primarily by fine-pebble breccia and associated calcrete that is developed on a micritic limestone that contains cryptalgal structures and is partially intraclastic (Stop 5). The most conspicuous disconformity manifests extensive karstification of a subaerial exposure surface and development of caverns beneath that surface (Stop 6). The third disconformity (also exposed at Stop 6) is marked by truncation of underlying strata and by at least one breccia-filled sinkhole.

LOCALITY DESCRIPTIONS, DAY 1

STOP 1, STE. GENEVIEVE LIMESTONE

Stop 1 is a road cut on State Road 135, 6.2 miles (10 km) south of I-64, SW¼ sec. 13, T4S R3E, Harrison County, Indiana. At this stop we will see most of the features used to deduce an eolian origin for some of the grainstone units. We will also evaluate the evidence for exposure surfaces. Most of the Ste. Genevieve is probably exposed at this locality (fig. 11), although the exact position of the base of the formation is unclear and the top is not exposed.

We begin at the northwestern end of this large road cut. The unit (unit I of fig. 11) exposed at road level at this point shows many of the features that are characteristic of eolian carbonates in the Ste. Genevieve. Note the evenly laminated, almost varvelike cross-beds, which occur mostly in sets 0.5-1.0 m thick. Careful observation of some of the laminae reveals an upward coarsening of grains and rarity of ripple foreset surfaces. Hand lens examination reveals scattered quartz sand grains and a variety of carbonate grain types. The unit contains no skeletal or other grains larger than about 2 mm.

After examining strata at the northwestern extremity of the cut, cross the highway very carefully and climb to the top of the east side of the cut. The top of this cut appears to be the crest of the dune of eolian unit I that we examined on the other side of the road. Note the sharp dune-crest line and the low-amplitude, relatively straight ripples on the upper surface of the bed. Most ripples are at right angles to the dune crest. Well-developed rhizocretions occur at places on the upper surface. They tend to follow specific laminae, perhaps corresponding to "looser," less well compacted horizons during growth of the plants. Look across to the larger cut on the opposite side of the road and identify the various units of the section. Especially note the lenticular shape of unit F. This eolian unit appears to be a dune that thins both to the north and to the south. Units G and H thin markedly over the dune crest.

After viewing the smaller, east cut, carefully recross the highway and view the section on the west side, toward the southern end of the cut. Unit E, which is exposed at this point, is a largely oolitic marine wackestone to grainstone. It contains scattered large invertebrate fossils, especially corals. Hand lens examination reveals that the grains are almost exclusively loosely packed ooids. The uppermost part of this unit contains a few possible vertical rhizomorphs and is brecciated in places. The upper surface of this unit is an exposure surface, the base of the second sequence identified in the Ste. Genevieve in this region. Note the

well-developed rounded pebbles in the lower few cm of the overlying unit F. The origin of these pebbles is not clear. They may be a thin alluvial gravel produced by sheet flood, perhaps during storms, as water ran across a poorly cemented upper surface of unit E. Or, they may have formed as a lag deposit produced by waves or currents on the shore of the retreating sea. Pebble zones are common at the base of this and other eolian units elsewhere. Next, climb upward and toward the north through marine units G and H and eolian unit I. A few rhizocretions can be observed near the upper surface of unit I. Marine trace fossils (*Zoophycos*?) occur in the uppermost part of unit I, suggesting that marine flooding occurred over the surface of the unlithified eolian unit. The lower bench upon which we are walking is cut at the top of unit I. Lagoonal or intershoal marine carbonates of units L and M are exposed in the cliff face (Units J and K do not occur in this exposure). If time permits, you may wish to climb higher up the cut to see the overlying units, including unit N, which is the uppermost eolian unit exposed in the cut. The uppermost part of unit M is extensively brecciated as the result of subaerial exposure before deposition of the overlying eolian unit.

Unfortunately, the contact between units M and N is difficult to view at this locality. Marine units O through R, which range in lithology from mudstone to grainstone, are exposed in the upper part of the cut. Unit R, an echinodermal rudstone to grainstone, is especially distinctive.

STOP 2, ST. LOUIS AND STE. GENEVIEVE LIMESTONES

Stop 2 is a road cut on State Road 135, 2 miles (3.4 km) south of I-64, in sec. 35, T3S, R3E, Harrison County, Indiana. Most of the features seen at Stop 1 are also visible at this stop. Exposure features and small-scale structures of the eolian units are well exposed. The section exposed in this cut (fig. 12) is almost identical to that at Stop 1 except the lower part of the section is better exposed here. The position of the contact between the St. Louis and Ste. Genevieve Limestones is not well defined but, depending on the criteria used to recognize it, probably lies near the base of the section exposed in this large cut. Unit R is the uppermost unit exposed in this cut, just as it is at Stop 1.

At the south end of the east side of the cut, unit A (fig. 12) is the lowest unit exposed. Note the abundant chert nodules in the skeletal packstone to grainstone. This is the Lost River Chert, which is included in the upper part of the St. Louis Limestone by current practice of the Indiana Geological Survey. Some other surveys and researchers include this interval within the lower part of the Ste. Genevieve. Overlying unit A is a thin unit (unit B) consisting of skeletal grainstone to rudstone that varies considerably in thickness on a local scale. Note the wavy nature of the upper contact of this unit. We interpret unit B as being deposited by marine storm currents. A 3-m-thick interval (units C and D) consisting mostly of fine-grained dolomite overlies unit B. An irregular scoured surface within unit C can be clearly seen at this stop. A discontinuous ooid grainstone occurs in low spots on this scoured surface. The rocks beneath this surface are brecciated in places. We interpret this surface as one that formed during a short period of subaerial exposure. The grainstone pods are probably reworked marine sands. A marine origin for the scoured surface cannot be disproven, but the widespread

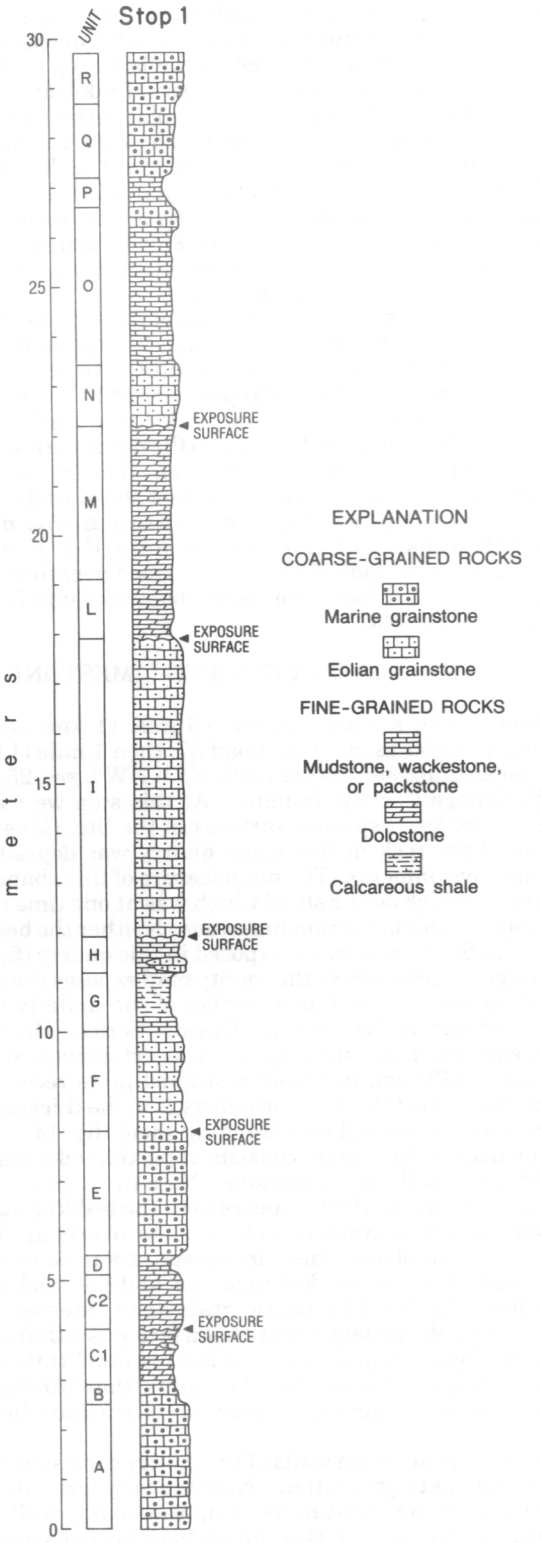

FIGURE 11.—Graphic column of Ste. Genevieve Limestone exposed in road cut on State Road 135 at Stop 1. Units A and B are based on adjacent exposures. Measured section for this stop is in Appendix.

occurrence of the surface throughout the area supports the subaerial exposure interpretation. Oolitic wackestone to grainstone of unit E (observed at the last stop as well as here) forms the light-colored unit above the dolomitic interval. The Indiana Geological Survey places the base of the Ste. Genevieve at the base of unit E. The lower bench on the east side of the road is cut at the top of unit E. Large coral colonies (*Syringopora*) clearly prove a marine rather than eolian origin for this unit. Most of the low vertical surface above the bench consists of eolian unit F, which displays well-developed eolian cross-bedding. Brecciated, chert-rich unit G forms the top of this exposure.

Northward toward the main part of the cut, the contact between marine unit E and eolian unit F is exposed at road level and appears much as it did at Stop 1, including well-developed pebbles in the basal part of unit F. Units G and H are at road level along the low slope to the north. At the north end of the cut, unit I makes up the top of the low bench and unit H is exposed at road level. The rhizomorphs preserved in the upper part of each of these units evince exposure to root penetration both before and after deposition of the eolian unit. Four eolian units (F, I, K, and N) occur on the east side of this cut. A good overview of the section can be obtained from the low bench (on unit I) on the west side of the cut.

STOP 3, STE. GENEVIEVE LIMESTONE

Stop 3 is in a small quarry 0.6 mile (1 km) north of downtown Orleans on State Road 37, then 1 mile (1.6 km) west on an unnamed county road. NE¼ NW¼ sec. 25, T3N, R1W, Orange County, Indiana. At this stop we will see evidence for two exposure surfaces in the Ste. Genevieve, but all of the rock in this small quarry was deposited in marine environments. The main feature of this abandoned quarry is a thick oolitic shoal which was at one time mined as a source of high-calcium limestone. Neither the base nor top of the Ste. Genevieve is exposed in this quarry (fig. 13). The larger quarry across the county road exposes the entire Ste. Genevieve as well as a portion of the underlying St. Louis and part of the overlying Chester Series. The oolitic shoal exposed in the small quarry was extensively studied by Carr (1973) and has been restudied more recently by Dodd and others (1990a). The quarry is in the thickest part of the northeast-southwest-trending shoal (fig. 14).

The floor of the quarry consists of partially dolomitized mudstone to pelletal wackestone. Note the uneven, wavy nature of the floor, which appears to be the bedding surface between the fine-grained rock and the overlying oolitic grainstone. In places, this surface appears to be corroded and bored. It is also cracked in places, and the cracks have been partially filled by oolitic grainstone filtering down from above. We believe that this surface was lithified and fractured before deposition (or at least before lithification) of the overlying grainstone. We think that lithification probably occurred during exposure of the surface when sea level fell.

Practically all of the walls of the quarry consist of oolitic to skeletal-oolitic grainstone. Note the very large stylolite in the grainstone about halfway up the quarry wall. The lithology of the oolitic facies can perhaps best be viewed in the large blocks at the base of the wall. Some of the blocks contain large intraclasts. These come from near the top of the shoal and formed when marine sand was partially cemented, broken by storm waves, and rounded by marine waves and currents. Packing is generally looser in the upper part of the quarry, suggesting earlier marine cementation (before compaction by overburden) than in the underlying portion of the shoal.

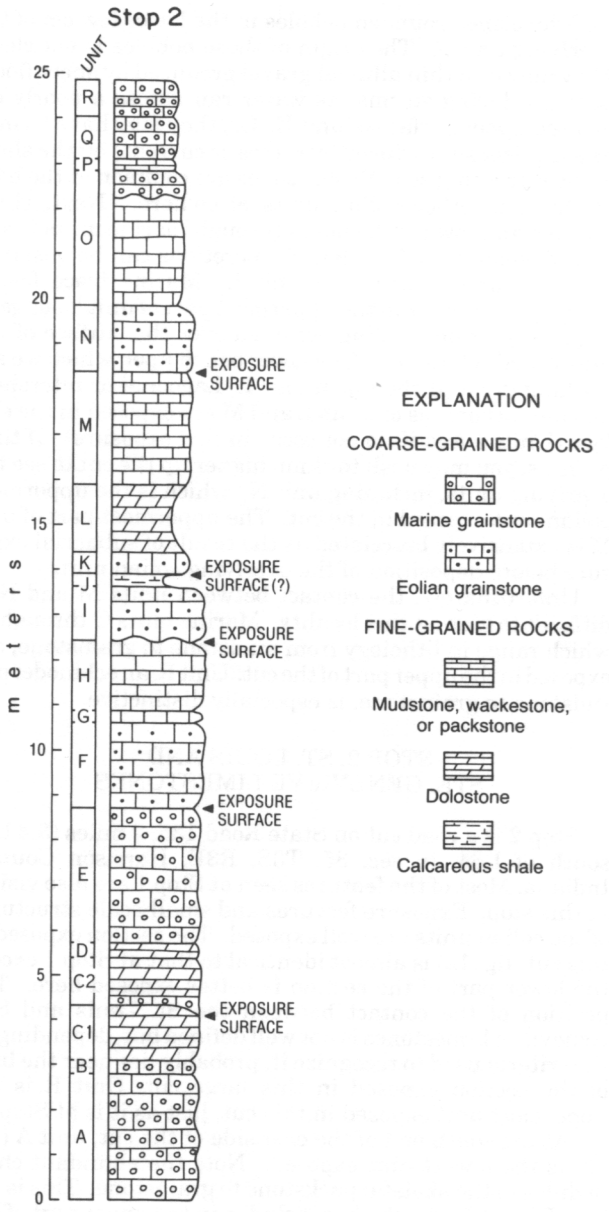

FIGURE 12.—Graphic column of St. Louis and Ste. Genevieve Limestones exposed in road cut on State Road 135 at Stop 2 (from Merkley, 1991). Measured section for this stop is in Appendix.

In order to see the upper part of the quarry, we will walk toward the county road and take a path to the top of the quarry. At the crest of the quarry the rock has been extensively brecciated. Unfortunately, the place to see this brecciation is difficult to get to and dangerous. We will have on display a sample which came from this interval. This brecciated horizon probably resulted from pedogenic processes, indicating that at least the crest of the shoal was subaerially exposed after its formation. About 4 m of mudstone and wackestone are found above the oolitic shoal. This interval was probably deposited in a lagoonal or intershoal area of the shallow Ste. Genevieve sea. Note the well-developed trace fossils (*Chondrites*) on bedding surfaces exposed in the highest part of quarry.

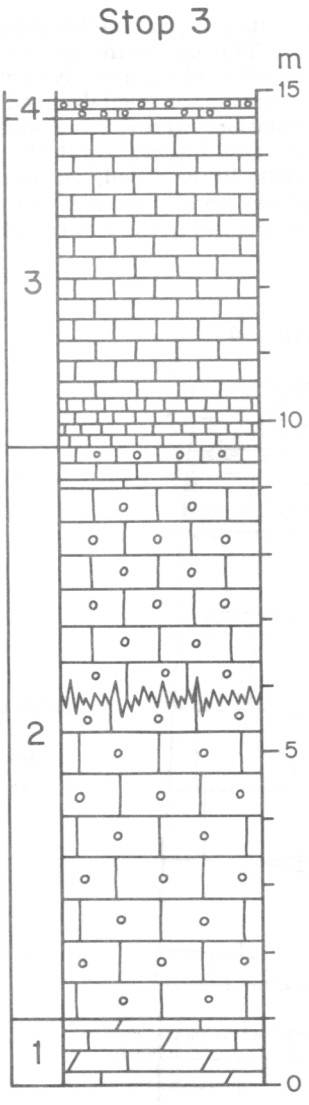

FIGURE 13.—Graphic column of Ste. Genevieve Limestone exposed in quarry at Stop 3. Symbols as in figure 12. Measured section for this stop is in Appendix.

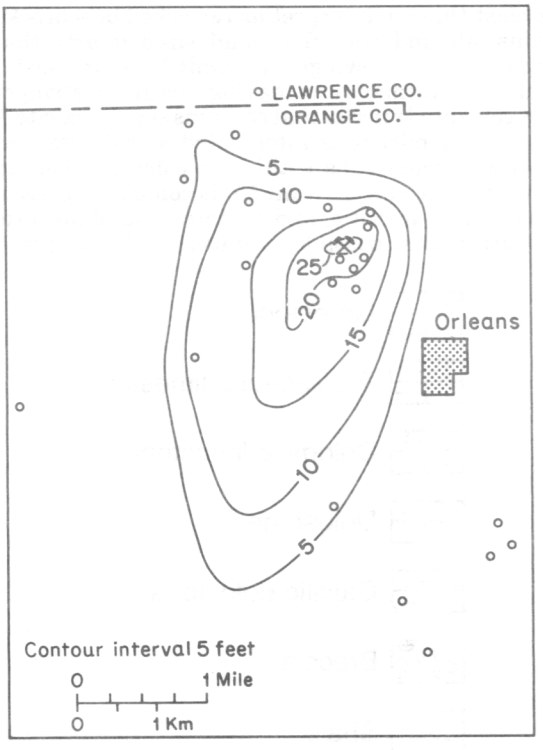

FIGURE 14.—Isopachous map of oolitic shoal exposed at Stop 3. Open circles are well locations.

LOCALITY DESCRIPTIONS, DAY 2

STOP 4, STE. GENEVIEVE LIMESTONE

Stop 4 is in a cut on the west side of State Road 37, 0.5 mile (0.8 km) north of the junction with State Road 60, W1/2 sec. 35, T4N, R1W, Lawrence County, Indiana. At this stop the stratigraphic section preserves sediments of an essentially classic offshore-shelf-to-subaerial-exposure sequence of depositional environments (figs. 15, 16). Unit 1 is the product of deposition in a normal-marine, high-energy offshore shoal-water environment analogous to that along the western edge of the Great Bahama Bank at Cat Cay (Ball, 1967). Units 3 and 4 contain fewer ooids and more skeletal grains than unit 1 and were deposited in an area of slightly lower energy that was transitional between the high-energy shoal and a mostly quiet-water, probably deeper water shelf lagoon (see Wilson, 1975; Enos, 1983). The presumed lagoon is represented by units 5 and 7, which consist predominantly of wackestones and packstones with bioturbated fabric. Biosparites and oosparites of unit 8 indicate reestablishment of a high-energy depositional environment that may have resulted from a small drop in relative sea level, establishment of a mid-lagoonal shoal, or migration into the area of a shoal-water bank. This event was succeeded by a return to quieter and probably deeper water lagoonal conditions during which the bioturbated packstones and wackestones of units 10 and 11 were deposited. Local patches of grainstone in these units signify occasional stirring of sediments by wave action in increasingly closer to shore depositional environments. Thinly interlaminated silty and sandy oosparite (fig. 17) of unit 13 is interpreted as a beach deposit. Unit 13 is locally trough cross-laminated, contains at least one

large clast that we interpret as reworked beachrock, and contains silt and very fine sand sized quartz that we interpret as windblown grains. Unit 14 is similar to unit 13, differing primarily in having irregular stringers of tightly cemented micrite that contains sparry-calcite-filled tubules. The micrite is interpreted as calcrete and the tubules as rhizomorphs within the calcrete. The uppermost unit of the section (unit 15) is complexly brecciated, predominantly micritic, and contains abundant birdseye vugs, intraclasts, possible pisoliths, and dense micritic limestone that contains spar-filled tubular alveolar structure (figs. 18-20). This unit is interpreted as a supratidal deposit that was affected extensively by pedogenesis that occurred when relative sea level dropped and large areas of the carbonate platform were exposed subaerially (Leibold, 1982). The brecciated interval (unit 15), known formally as the Bryantsville Breccia Bed, occurs at the top of the Ste. Genevieve Limestone in many areas of the southwestern Indiana outcrop and in the adjacent part of Kentucky (Malott, 1952).

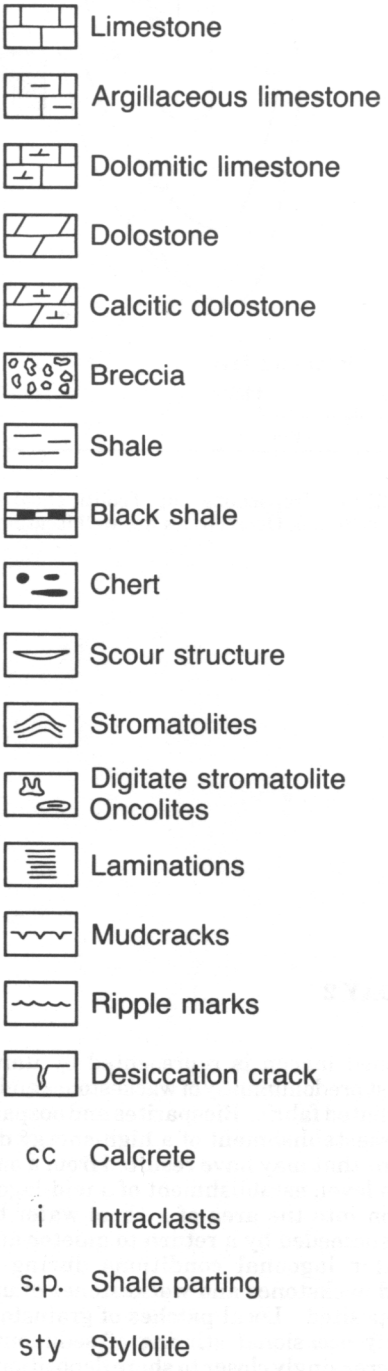

FIGURE 15.—Explanation of symbols used in graphic columns of rocks exposed at Stops 4, 5, and 6.

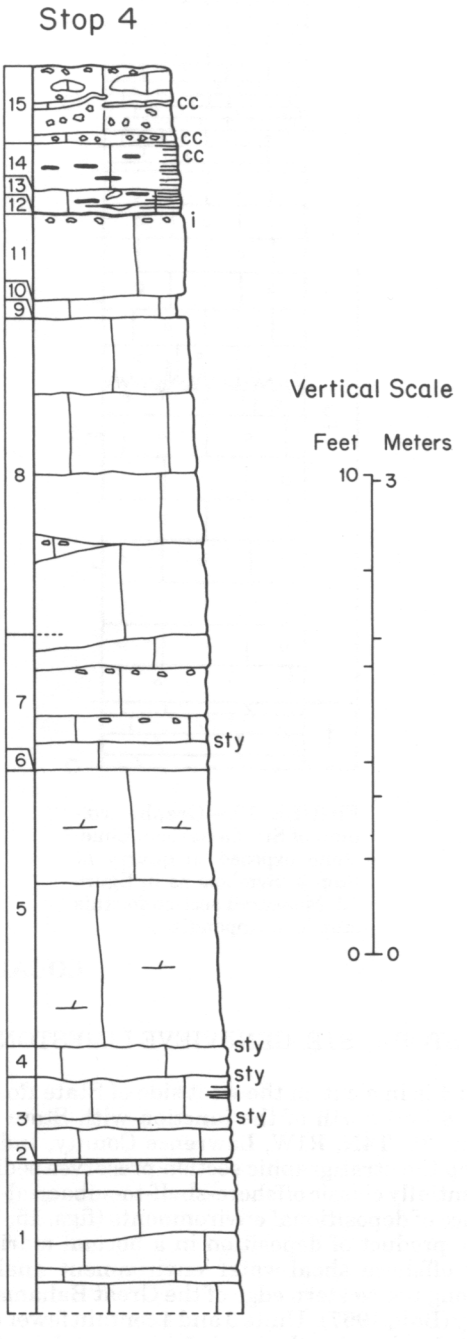

FIGURE 16.—Graphic column of upper part of Ste. Genevieve Limestone exposed at Stop 4. See figure 15 for explanation of symbols. Measured section for this stop is in Appendix.

FIGURE 17.—Laminated beach sand in unit 13, Stop 4. Note alternation of coarse and fine laminae. Plane-polarized light, X20.

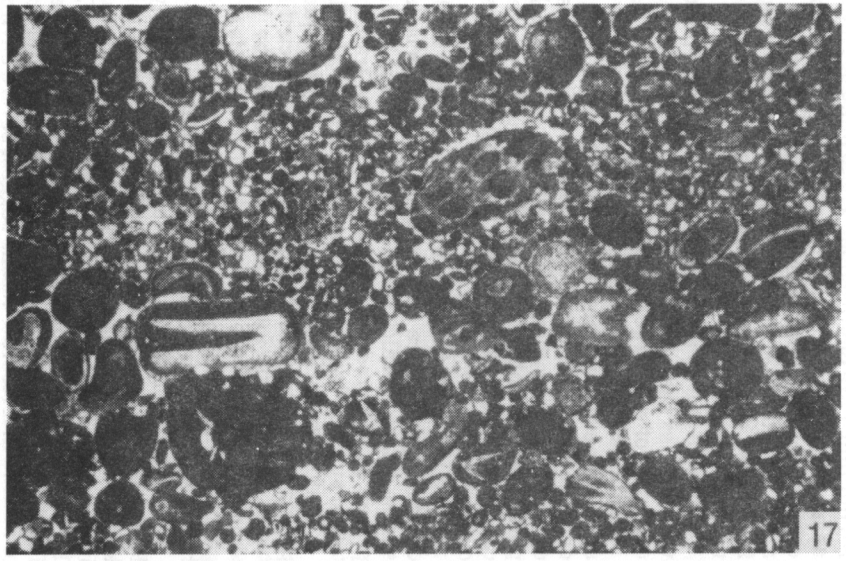

FIGURE 18.—Supratidal rock that has been affected by pedogenesis. Note brecciated texture and alveolar structure near center. Unit 15, Stop 4. Plane-polarized light, X20.

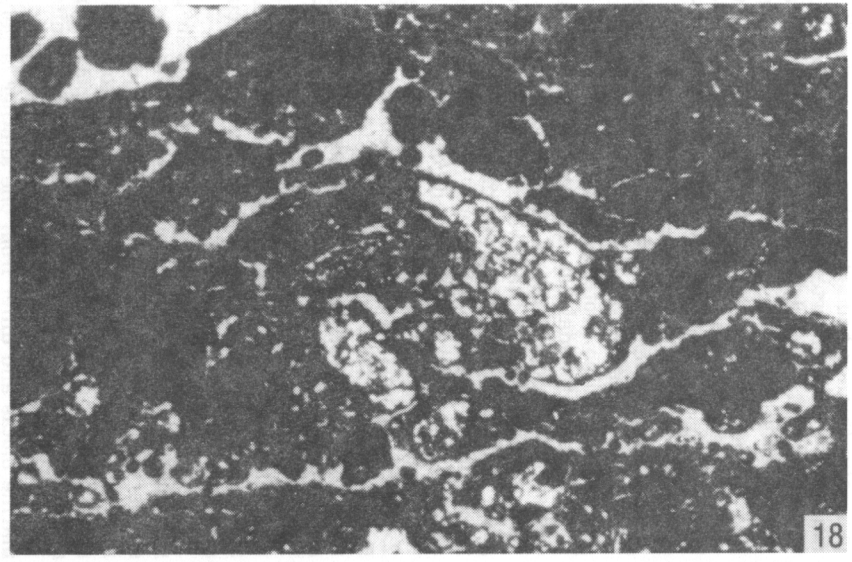

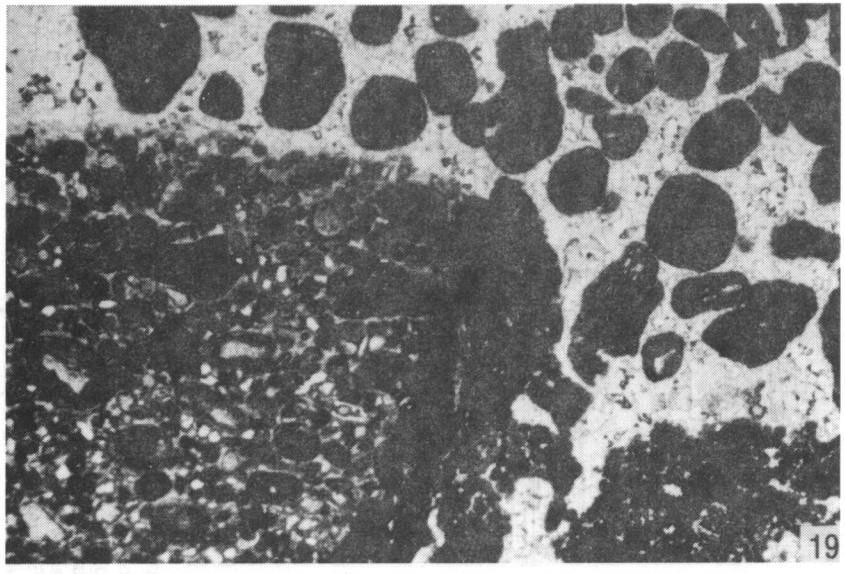

FIGURE 19.—Supratidal rock that has been affected by pedogenesis. Note clasts in birdseye structure and bit of calcrete crust on right side of clast (lower left) of mixed-grain packstone. Unit 15, Stop 4. Plane-polarized light, X20.

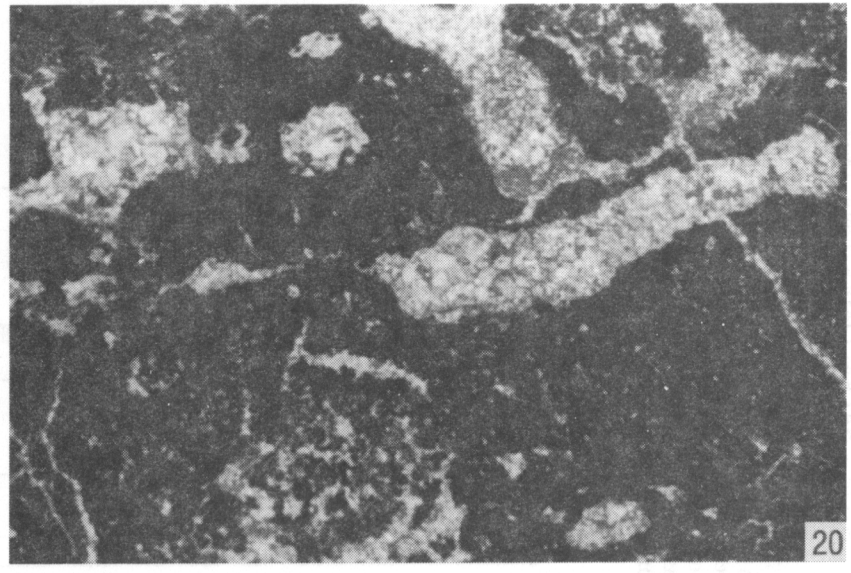

FIGURE 20.—Supratidal rock with birdseye structure that has been brecciated during pedogenesis. Unit 15, Stop 4. Plane-polarized light, X20.

STOP 5, SALEM LIMESTONE AND ST. LOUIS LIMESTONE

Stop 5 is a cut on the east side of State Road 37 at the junction with State Road 58 West, SW¼ sec. 32, T6N, R1W, Lawrence County, Indiana. Greenish-gray shale composed mainly of illite and reaching thickness as great as 0.5 m serves as a useful marker that separates thicker bedded grainstones and packstones of the Salem Limestone from

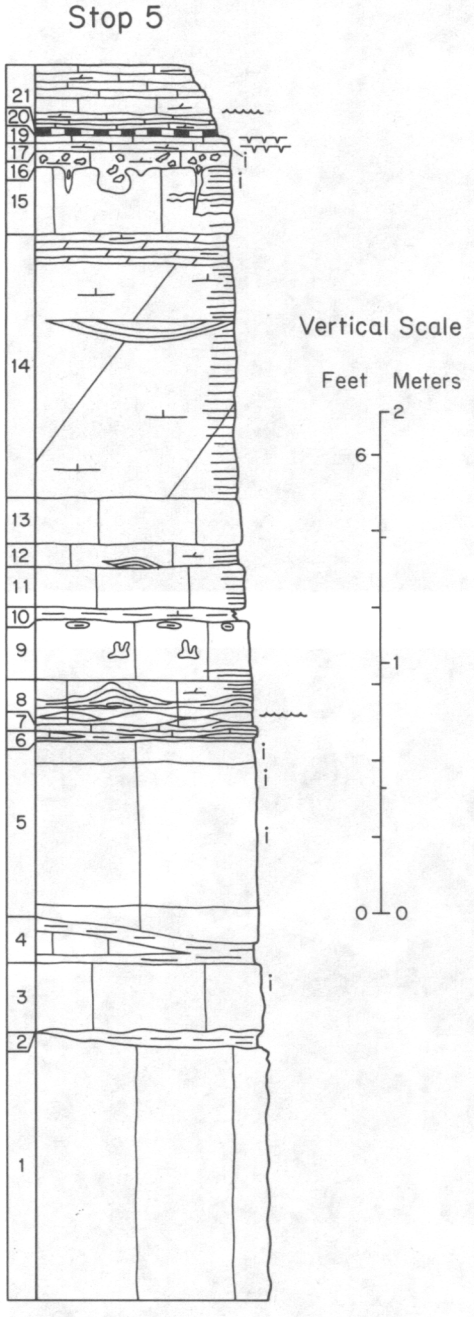

FIGURE 21.—Graphic column of uppermost bed of Salem Limestone (unit 1) and lower part of St. Louis Limestone (units 2-21) exposed at upper end of road cut at Stop 5. Unit 18 is a shale parting too thin to plot at this scale. See figure 15 for explanation of symbols. Measured section for this stop is in Appendix.

generally thinner bedded packstones, wackestones, and mudstones that characterize the lower St. Louis interval. The shaly unit is widely developed along State Road 37 in the field-trip area, and is best interpreted as a blanket of fine-grained siliciclastic detritus that was derived from easterly source lands and was dispersed across the Valmeyeran carbonate platform during a major storm. This shale bed signals development of a genetically related group of more or less restricted depositional environments that included normal-marine protected shelf (or open lagoon), hypersaline protected shelf (or restricted lagoon), hypersaline intertidal flat, supratidal flat, and subaerial exposure. Predominance of packstone, wackestone, and mudstone textures in the lower part of the St. Louis suggests that most carbonate sediments were deposited in moderate- to low-energy settings. Several beds contain a severely restricted paleobiota and/or stromatolitic structures that suggest episodes of hypersalinity. Indeed, just 2.4 miles (3.8 km) north of Stop 5, a bed equivalent to unit 5 (fig. 21) contains millimeter-scale voids that suggest intrastratal dissolution of small evaporite nodules; 20 miles (32 km) to the southwest, lower parts of the subsurface St. Louis are marked by commercial deposits of gypsum. Thus, in the area at and surrounding the section at Stop 5, a substantial part of early St. Louis deposition occurred at salinities that were elevated well above normal.

For convenience of discussion, beds at Stop 5 are grouped according to shared features which derive from the same or similar environment of deposition. These groups are treated in order of environmental progression, from offshore to supratidal. The measured section (See Appendix) includes several predominantly packstone/wackestone units (units 1, 3, 9, 11) that contain abundant and moderately diverse marine biotas and differ from one another largely in the character and relative proportions of allochemical grains. All but unit 1 are bioturbated. These units are interpreted as normal-marine subtidal deposits of a low- to moderate-energy protected shelf or open lagoon. Intraclasts near or at the top of units 3 and 11, and oncolites near the top of unit 9, suggest that each of these beds reflects shallowing-upward deposition.

Units 13 and 19 are bioturbated biomicritic packstones/wackestones that contain low to very low diversity biotas composed of very large numbers of ostracodes (fig. 22). Unit 13 contains a few intraclasts, and unit 19 has mud cracks on at least one bedding surface. Apparently, both units were deposited in a very restricted shallow-water, occasionally emergent environment such as a lagoon in which some parameter, probably hypersalinity, served to reduce drastically the biotic diversity and thus foster proliferation of ostracodes.

Unit 17 is a bioturbated mudstone that has mud cracks on the upper surface and contains local intraclasts and a sparse ostracode-calcisphere paleobiota. This bed is interpreted as the product of deposition in the transition between subtidal hypersaline lagoon and intertidal flat.

Unit 5 comprises a shallowing-upward sequence of pelletal intrasparrudite that contains a restricted marine biota and micritic intraclasts characterized by birdseye structure. Textures, biota, and structures of this unit suggest deposition during transition from a shallow-water, hypersaline lagoon to supratidal conditions.

Some beds consist of mostly laminated and locally cross-laminated or scoured micritic mudstones that contain crinkly horizontal to mounded cryptalgal structures and few invertebrate body or trace fossils. These beds, units 7, 8, 12, 14, and 15, are here interpreted as products of intertidal-flat deposition (fig. 23). The limited number and diversity of marine invertebrate fossils suggest severe environmen-

FIGURE 22.—Bioturbated biomicritic packstone in which preponderance of grains is ostracode valves. Unit 13, Stop 5. Plane-polarized light, X20.

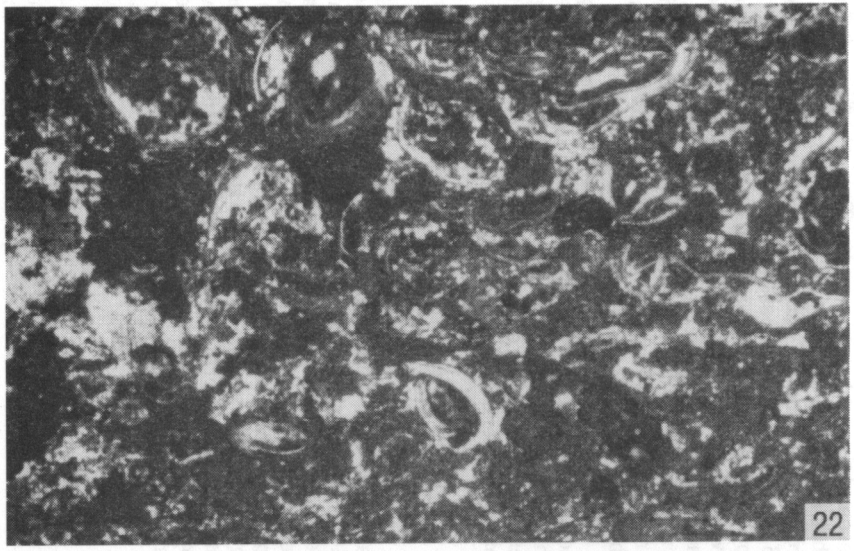

FIGURE 23.—Micritic limestone containing crinkly structures that are interpreted as stromatolitic laminae. Unit 7, Stop 5. Plane-polarized light, X20.

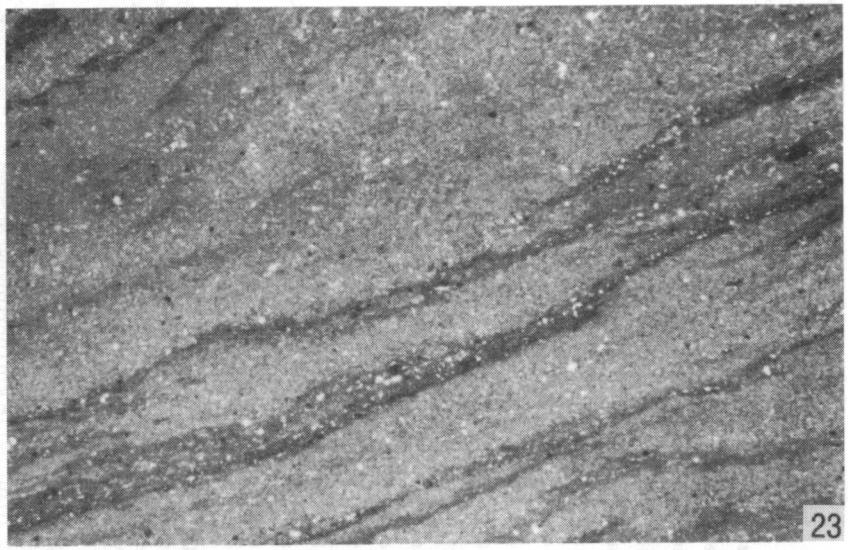

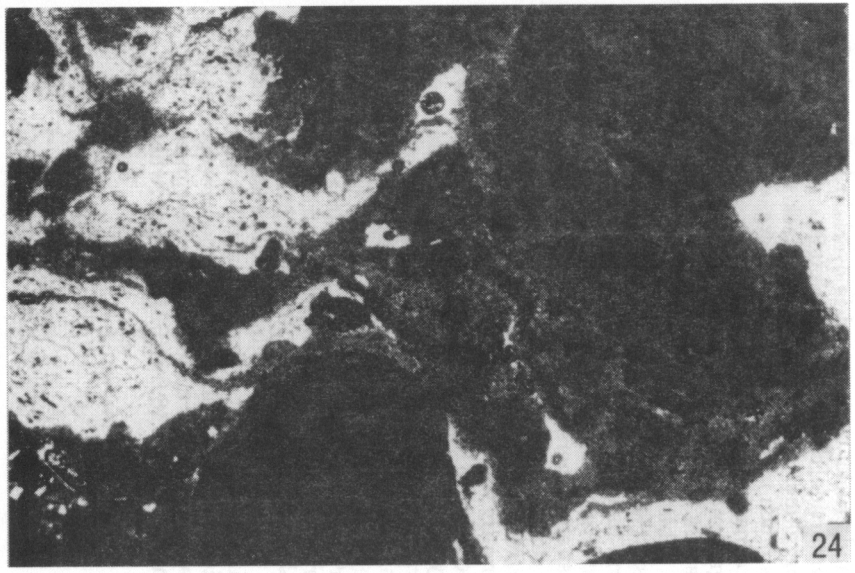

FIGURE 24.—Calcite-cemented pedogenic breccia in unit 16, Stop 5. This unit also contains tightly cemented micrite (calcrete) and local alveolar structure. Plane-polarized light, X20.

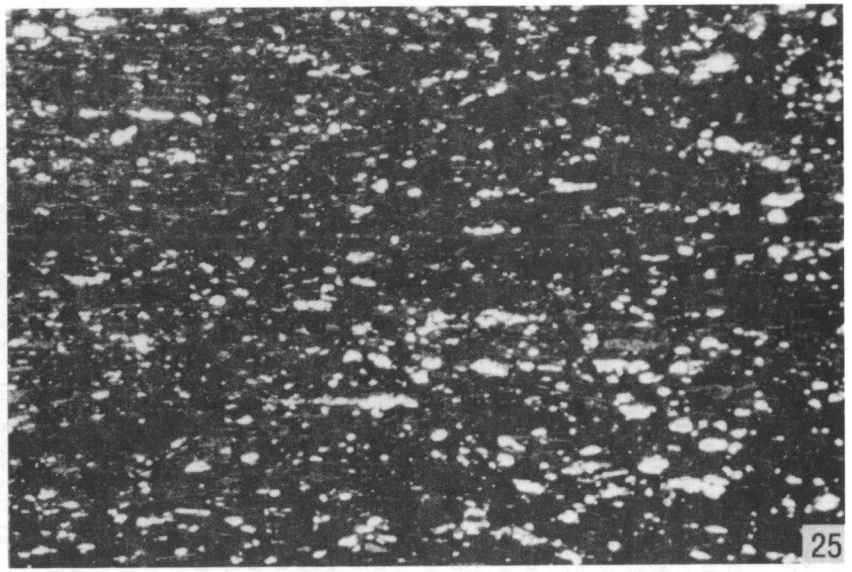

FIGURE 25.—Organic-rich black shale (marine coal) showing well-laminated structure. Black areas are amorphous organic material; slightly lighter colored grains and wisps are fragments of algae according to Dembicki and others (1976) and Aureal Cross (oral commun., 1985). Unit 20, Stop 5. Plane-polarized light, X40.

tal restriction, and the presence of stromatolitic structures suggests strongly that this restriction was caused by hypersalinity. Unit 14 apparently lacks cryptalgal structures at Stop 5 but does contain crinkly cryptalgal structures near the top in sections exposed 2.4 and 4.4 miles (3.8 and 7.0 km) to the north. Unit 14 also contains small, rounded stromatolites near the base of the section that is exposed 4.4 miles to the north. Bundling of laminations within unit 14 may have resulted from tidal influences.

Unit 21 also lacks cryptalgal structures but is otherwise well laminated and contains sparse ripple marks and little evidence of fossils. In the section exposed 2.4 miles to the north this unit has mud cracks, and in a section exposed 4.4 miles to the south the unit has mud cracks and in situ brecciation. Unit 21 therefore appears to have been deposited at the intertidal/supratidal boundary.

Combinations of features such as mud cracks, layers of intraclasts, birdseye structure, mechanically produced laminations, and cryptalgal laminations characterize the supratidal environment (*e.g.*, Shinn, 1983; Sarg, 1988), which is the depositional setting we conclude for unit 15 at Stop 5. This unit is capped by an irregular crust (unit 16) consisting of micrite-cemented fine-pebble breccia that extends irregularly downward into fractures in unit 15 (fig. 24). Lithology, texture, geometry, and presence of minute calcite-filled rhizocretions confirm a subaerial-exposure environment for this unit.

An important organic-rich grayish-black shale, unit 20, lies between beds here interpreted as shallow-water hypersaline-lagoon (unit 19) and intertidal deposits (unit 21). The black shale is relatively rich in fish bones, teeth, and scales, contains sparse disarticulated brachiopod valves (one species), and contains disseminated grains of quartz silt (fig. 25). At the road cut 2.4 miles north of Stop 5 the black shale is underlain by an intertidal stromatolite bed that has mud cracks on top, and is overlain by a bed of laminated intertidal carbonate rock that has mud cracks on one bedding plane. The organic-rich black shale, which contains as much as 53 weight-percent organic carbon, is essentially a marine coal. We interpret this unit as a pile of marine algae and other organic matter that was heaped along the shore of a hypersaline lagoon during a severe windstorm. This storm also accounts for the abundance of quartzose silt (wind-blown) and for disarticulation of brachiopods and fish that were washed into the hypersaline environment from farther offshore (Dembecki and others, 1976; Nellist and others, 1985). A Devonian spore (Aureal Cross, oral commun., 1986) was discovered in a sample of black shale from the road cut 2.4 miles north of Stop 5. This spore apparently was blown to the site from an area where Devonian rocks were being eroded. Only one conodont was recorded by Nellist and others (1985). This shale unit shares characteristics of both nearshore and offshore black shales as characterized by Coveney and others (1991) but is clearly a nearshore deposit.

An environmental plot of the foregoing interpretations reveals marked cyclity (fig. 26) that differs from that documented by Jorgensen and Carr (1973) both in scale and by absence of gypsum beds. Bagby (1989) recognizes four cycles within the lower part of the St. Louis that are defined by alternation of environment similar to those recognized at Stop 5. However, the four cycles that she recognizes occur within an interval that is 18.9 m (62 feet) thick, whereas the

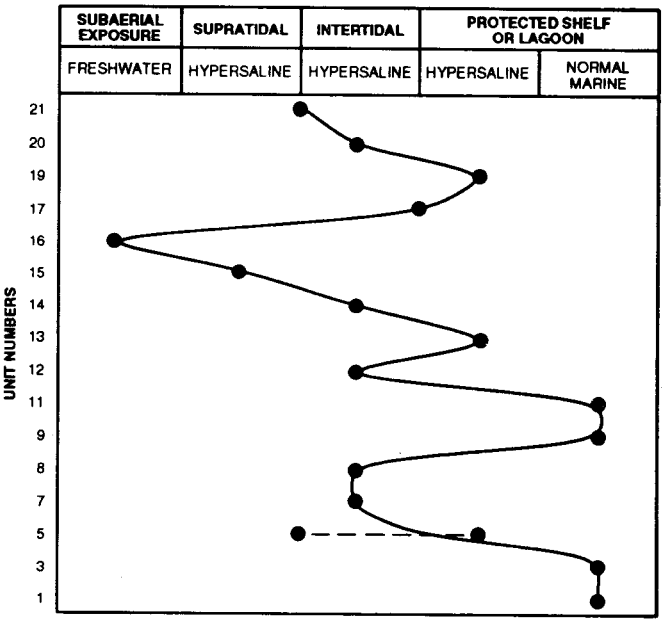

FIGURE 26.—Depositional cyclicity manifest in stratigraphic section exposed in road cut at Stop 5. Clayey shale beds not included. Points for unit 5 indicate wide range of possible depositional environments represented by this interval.

3 1/2 cycles shown in figure 26 occur within an interval of only 5 m (16.2 feet), and the core that she studied was taken just 10 miles (16 km) northwest of Stop 5. Direct correlation of the cyclicity at Stop 5 with that of Bagby is not likely. Research has not progressed sufficiently far to define possible causes of cyclicity in the section at Stop 5. The prolonged episode of subaerial exposure indicated by unit 16 is recognizable across a several-county area of the St. Louis outcrop of Indiana and strongly suggests a drop of sea level rather than local uplift. The association of evaporites, stromatolites, and calcrete in the lower part of the St. Louis at and adjacent to Stop 5 suggests deposition under climatic conditions of semi-aridity (See Esteban and Klappa, 1983; Choquette and James, 1988; Ettensohn and others, 1988).

The origin of thin shale partings within the lower part of the St. Louis, including units 2, 4, 6, 10, and 18, is uncertain. The siliciclastic nature of these shales denotes terrigenous detrital sources, but direction and mode of transport have not been determined.

STOP 6, ST. LOUIS LIMESTONE

Stop 6 is an exposure of the St. Louis Limestone in the wall of a canyon cut by McCormick's Creek in NW¼ sec. 23, T10N, R3W, McCormick's Creek State Park, Owen County, Indiana. McCormick's Creek has cut a canyon into carbonate rocks of Valmeyeran age. On the basis of conodont biostratigraphy, Carl Rexroad (oral commun., 1991) assigns the entire section at Stop 6 to the St. Louis Limestone, but John Droste (oral commun., 1992) considers at least the upper part of the section to be part of the Ste. Genevieve Limestone. The section at Stop 6 was measured at three

places along the wall of the McCormick's Creek canyon. These are referred to as Stops 6a, 6b, and 6c. Stop 6a is farthest downstream and is situated 80 m (260 feet) northwest of 6b. Stop 6c is situated approximately 300 m (985 feet) upstream from Stop 6b. All are approached by way of a cliff path that can be reached from the parking area at Echo Canyon shelter. Midway up the canyon wall at Stop 6a the stratigraphic section is interrupted by a conspicuous disconformity along which local relief is as great as 2.8 m (9 feet), and beneath which the section manifests textural and structural features that evince a major episode of subaerial exposure and karstification of emergent marine sediments.

At Stop 6a the measured section is 8.5 m (28 feet) thick (fig. 27). The lower 6.7 m (22 feet, 82%) of the section consists predominantly of micritic or microsparitic dolomitic limestone with mudstone texture. The remainder of this lower part is divided almost equally between limestone and dolostone, which are also composed predominantly of micritic or microsparitic mudstones. Nearly all of these units are massive, several have bioturbated texture (fig. 28), and several consist wholly or in part of solution breccia (fig. 29). Three of the units (units 2, 8, 16) include biomicritic wackestone and/or packstone textures, and one (unit 8) contains a small amount of grainstone. Marine trace or body fossils are recognized in more than half the carbonate-rock units within this 6.7-m interval. These rocks were deposited primarily in low-energy marine environments that ranged from near-normal salinity to hypersaline. Evidence of intertidal or supratidal deposition is not apparent.

(text continues on p. 21)

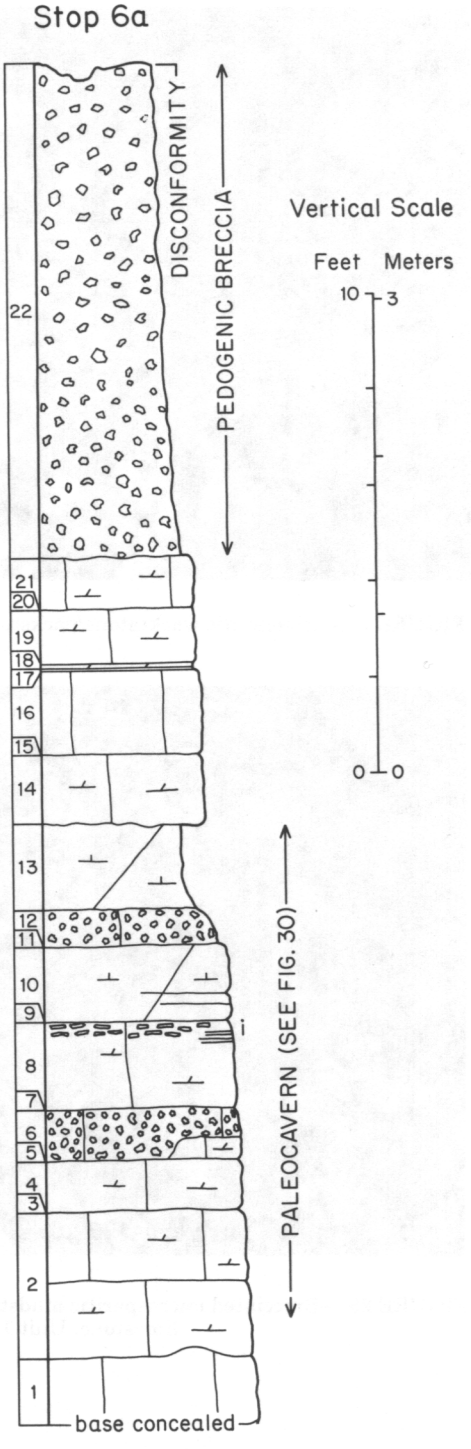

FIGURE 27.—Graphic section of St. Louis Limestone exposed at Stop 6a. Section was measured just to left of cliff-face cross section depicted in figure 30. See figure 15 for explanation of symbols. Measured section for this stop is in Appendix.

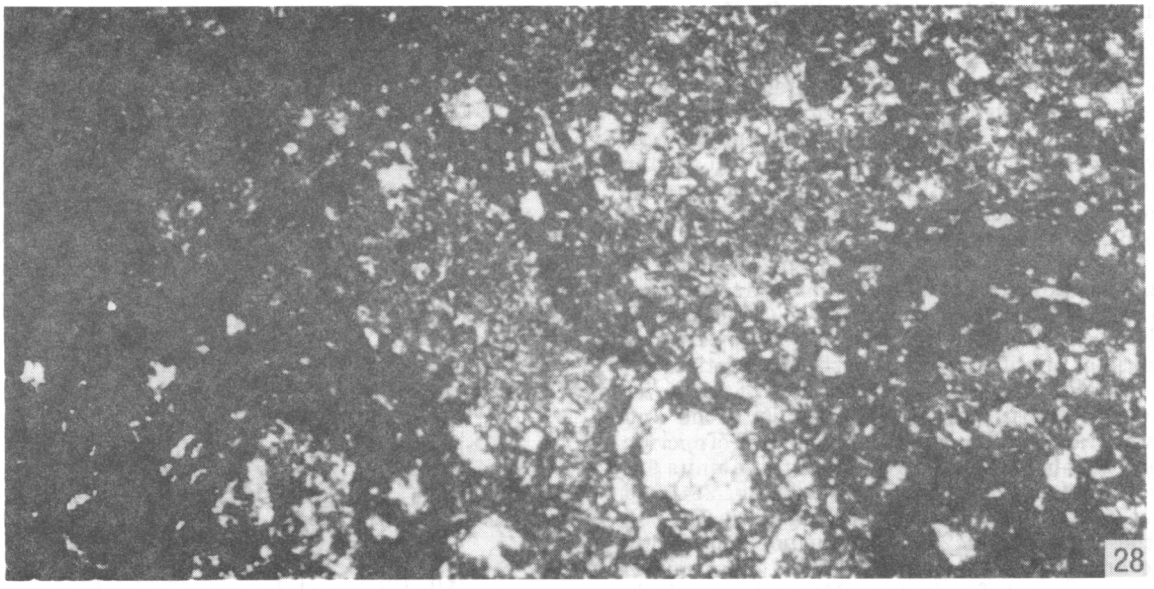

FIGURE 28.—Biomicritic wackestone/packstone that has pronounced bioturbated texture. Unit 16, Stop 6a. Plane-polarized light, X20.

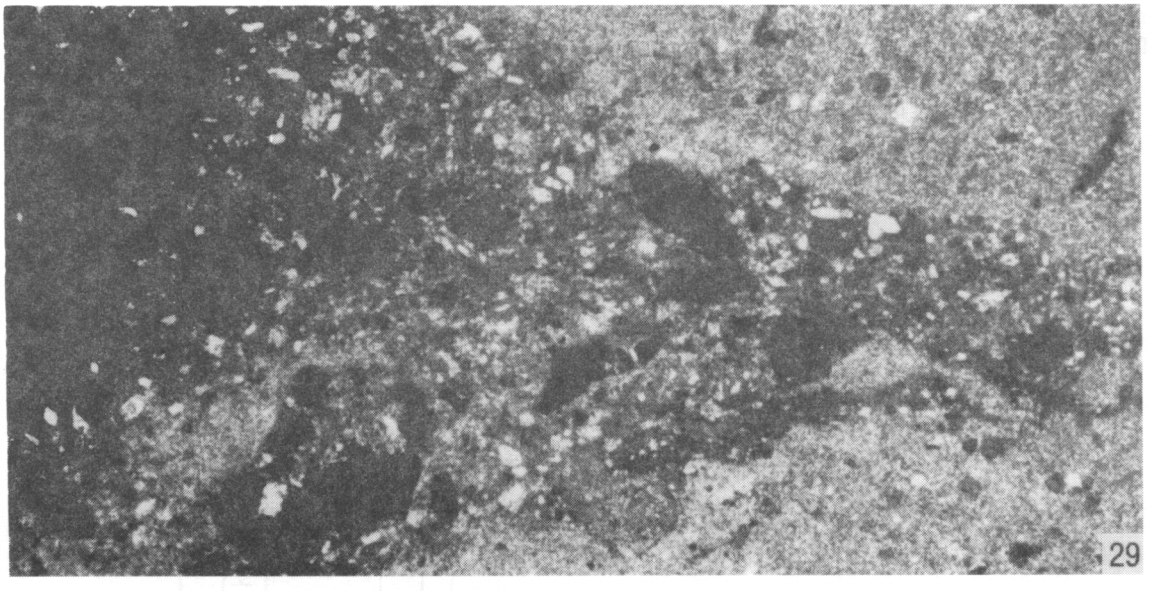

FIGURE 29.—Brecciated microsparitic mudstone bound by micritic matrix that contains minute clasts of micritic limestone. Unit 12, Stop 6a. Plane-polarized light, X20.

Within the lower 6.7-m interval are two large well-circumscribed bodies of angular-block breccia as much as 9 m (30 feet) wide and 5 m (16.5 feet) thick (fig. 30). Apparently, both of these are overlain and bordered laterally by essentially undisturbed beds of carbonate rock, and one of them is underlain by such rock. The breccias are bound by a matrix of nonresistant medium-greenish-gray calcitic dolostone/dolomitic limestone that itself contains small angular carbonate-rock clasts and extends laterally as a 0.5-1 m (1.6-3.3 feet) thick bed connecting the two large breccia masses. These two breccia bodies are interpreted as paleocaverns (Hattin and Swain, 1990a, 1990b) that were formed during karstification of the emergence surface now represented by the disconformity (fig. 30). These caverns were filled partly by blocks that fell from the cave walls and ceiling and partly by carbonate mud that was flushed into the cavern system when the overlying karstic land surface was reinvaded by the sea. The mudstone (unit 13) fills a low-ceilinged crawl space that connected upper parts of the two cavern passageways, and was filled mainly by flushed-in mud rather than by fallen blocks.

At Stop 6a the measured section is capped by as much as 3.1 m (10 feet) of nonstratified pebble/cobble breccia consisting of limestone and dolomitic limestone clasts that are set in a poorly sorted finer grained carbonate matrix. This bed wedges out laterally to the southeast along the canyon wall. This breccia, which directly underlies the disconformity, is interpreted as pedogenic, partly on the basis of position below the disconformity, occurrence of abundant alveolar structures (figs. 31, 32) in the underlying bed (unit 21), and occurrence of numerous small breccia-filled sinkholes (or dolines) and other pedogenic features in the same stratigraphic interval at Stop 6b.

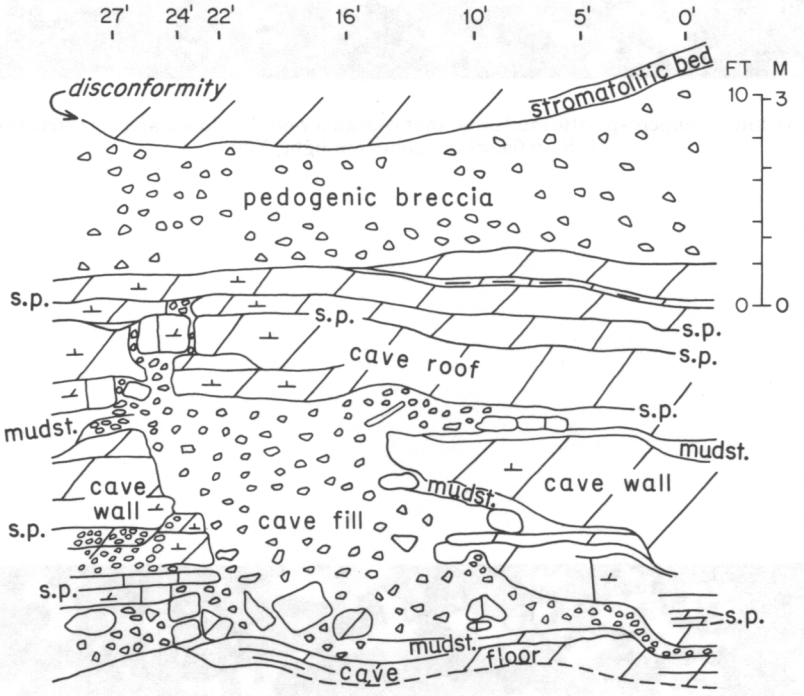

FIGURE 30.—Cross section of St. Louis Limestone in cliff face adjacent to measured section at Stop 6a depicted graphically in figure 27. Large body of breccia fills Valmeyeran paleocavern. Cross section is based on seven sections, numbered at top of figure, measured by D. E. Hattin and S. H. Swain in 1989 and 1990. Mudstone midway up section is unit 13 of section in figure 27, and pedogenic breccia is unit 22.

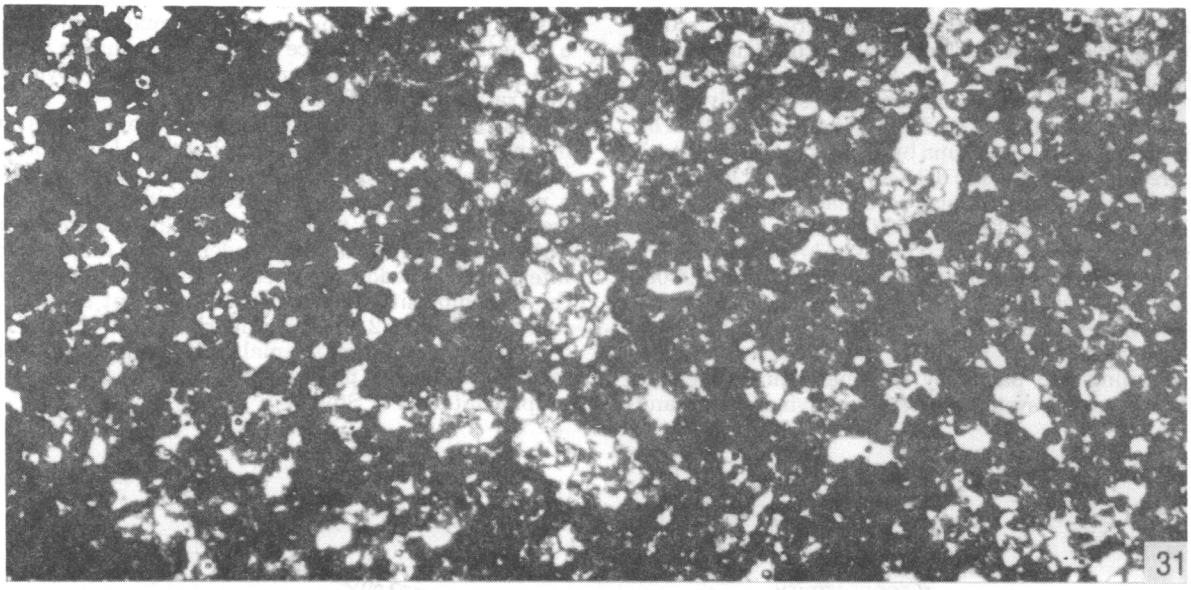

FIGURE 31.—Massive micritic/microsparitic mudstone that contains well-developed alveolar structure near center. Unit 21, Stop 6a. Plane-polarized light, X20.

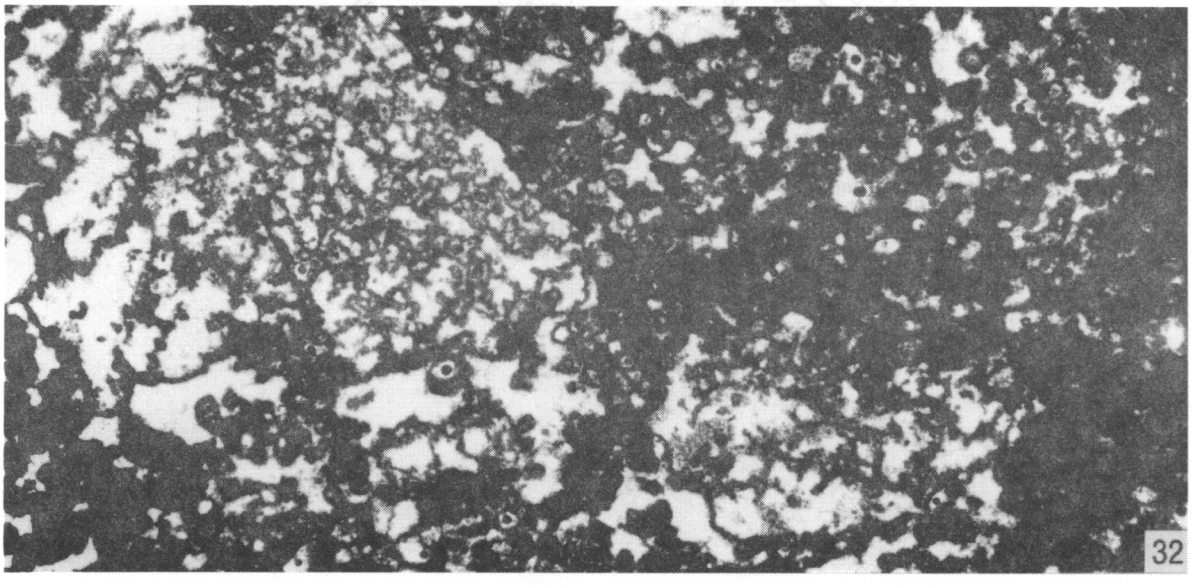

FIGURE 32.—Brecciated and sparry-calcite-cemented micritic limestone that contains abundant alveolar structure. Unit 21, Stop 6a. Plane-polarized light, X20.

High on the cliff faces at Stop 6a, a second stratigraphic discontinuity is evident. Truncation of strata and presence of a breccia-filled sinkhole-like feature beneath the break suggest that a disconformity was produced in this stratigraphic position during a second episode of Valmeyeran emergence (Hattin and Swain, 1990b).

At Stop 6b (fig. 33), the lower disconformity is delineated as the boundary between a stromatolite bed above and underlying rocks that contain much evidence of subaerial exposure, pedogenesis, and karstification. Most pronounced of the evidence are breccia-filled pits that are interpreted as sinkholes or dolines that developed on an emergent carbonate-rock surface and became filled with pedogenic breccia during weathering and erosion of the adjacent land surface (fig. 34) (Hattin and Swain, 1990a, 1990b). All along the adjacent cliff face at Stop 6b the stratigraphic section directly beneath the disconformity and laterally adjacent to the sinkholes has been more or less affected by solution and local brecciation and is further characterized by irregular, discontinuous lenses of greenish-gray mudstone that may be remnants of a gley soil (see Kahle, 1988; also, Frank Ettensohn, oral commun., 1991). Near the top of the most conspicuous pit at Stop 6b are pods of mottled greenish-gray/grayish-red mudstone composed of quartz, calcite, dolomite, illite, and kaolinite. These pods are interpreted as the result of pedogenesis in a zone affected by a fluctuating water table (see Kahle, 1988). At a single location on the cliff face, a small irregular-shaped body of carbonate rock that lies directly beneath the disconformity is cut by irregular pods of reddish-colored clayey mudstone that may be a remnant of terra rossa soil formed within the oxidizing zone of a soil profile.

(text continues on p. 24)

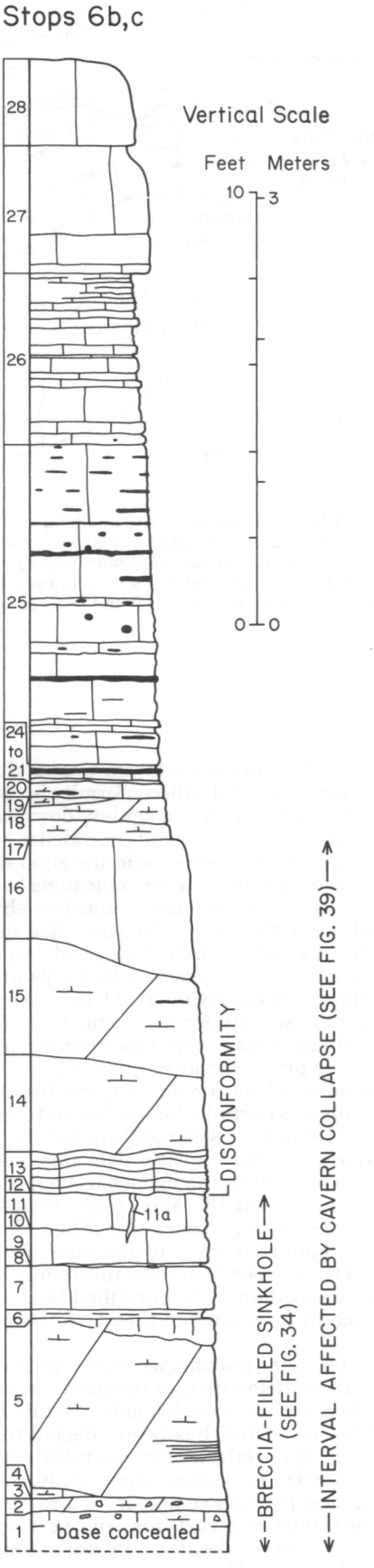

FIGURE 33.—Graphic column of St. Louis Limestone exposed at Stops 6b and 6c. See figure 15 for explanation of symbols. Measured sections for these stops are in Appendix.

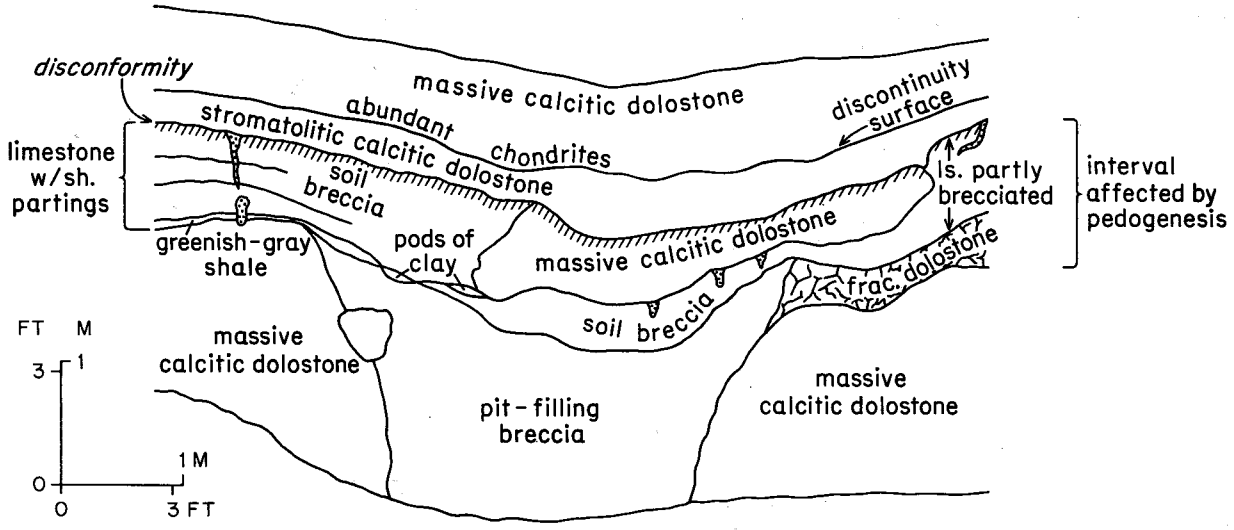

FIGURE 34.—Cross section of sinkhole (or doline) exposed beneath conspicuous disconformity that is widely traceable along canyon wall at Stop 6. Rock body labeled "massive calcitic dolostone" is filling of slight depression that remained on karstic land surface when the surface was reinundated by marine waters. Stromatolitic calcitic dolostone formed in hypersaline water in intertidal zone along edge of advancing sea. Cross section is based on 10 sections, measured at 2-foot intervals by D. E. Hattin and S. H. Swain in 1989. Left end of cross section is position of section depicted graphically as units 1-14 in figure 33.

All along the canyon wall from west of Stop 6b to Stop 6c the section beneath the disconformity is cut to a depth as great as 1 m (3 feet) by irregular, downward-tapering, dikelike bodies of microcrystalline calcitic dolostone that contain fragments of possible micritic algal structures and very sparse foraminifers. These dolostone bodies, of which there are several score, are truncated sharply by the stromatolite bed that lies on the karstified surface and are interpreted as sedimentary fillings of large desiccation cracks similar to those reported by Loope and Haverland (1988) from the Pennsylvanian of Utah. Masses of calcitic dolostone that are similar lithologically to the presumed fracture fillings occur on top of the breccia that fills some of the sinkholes preserved at Stop 6b (fig. 34). In the most conspicuous sinkhole (or doline), the top of the calcitic dolostone mass is partially laminated and overlain directly by the well-laminated stromatolitic bed (fig. 33, unit 13). Laminations in these calcitic dolostone bodies suggest initial development of the cyanobacterial mats that ultimately produced unit 13. Apparently, mud that filled the presumed desiccation cracks also filled shallow depressions that remained within the sinkholes, above the breccia fillings. These deposits are the initial marine sediments that were washed onto the karstified land surface as the sea once again transgressed this part of the Valmeyeran shelf.

At Stop 6b, unit 5 is a conspicuously light-colored, mostly massive calcitic dolomite that becomes coated with silt- to fine- sand-sized clusters of dolomite crystals during weathering. The entire unit has been affected to a greater or lesser degree by the effects of intrastratal solution, producing a microbrecciated texture. Apparently, this process has destroyed most primary sedimentary structures, but a few laminations, burrow structures, and very sparse marine fossils are preserved locally. Predominantly mudstone texture and paucity of fossils suggest a somewhat restricted low-energy environment of deposition. The top of unit 5 is a tightly cemented dolomitic mudstone or microcrystalline dolostone that has been extensively brecciated (fig. 35).

Between unit 5 and the disconformity, three limestones (units 7, 9, 11) consisting mostly of biomicritic or pelmicritic wackestones/packstones (figs. 36, 37) contain relatively diverse biotas that bespeak deposition in a low- to moderate-energy normal- or nearly normal-marine protected shelf or open lagoon. At various places along the cliff face these three units bear evidence (wisps of greenish-gray clay, partial brecciation, slickensides) of pedogenesis.

The process of emergence and karstification documented in the foregoing paragraphs was succeeded by gradual submergence of the karstified land surface. As the sea advanced across this surface, carbonate muds were washed into desiccation cracks and residual depressions above sinkholes or dolines to produce disjunct bodies of what is now calcitic dolostone. This initial depositional event was followed at Stop 6b by establishment of an environment favorable to the extensive development of cyanobacterial mats, which trapped successive increments of sediment that are now preserved conspicuously as unit 13 (fig. 38). Most likely, that environment was the hypersaline intertidal zone of the advancing sea. Laterally, to the south of Stop 6b, the stromatolitic bed terminates abruptly against a topographic high formed by rock lying beneath the disconformity. This high is interpreted as a mound of bedrock within the intertidal zone. This local high on the karstified land surface was eventually buried by sediments of units 14 and 15, which are massive micritic to microsparitic calcitic dolostones/dolomitic limestones with mudstone texture. The lower part of unit 15 is riddled with burrows, some of which extend downward into the stromatolitic unit. A few recrystallized marine fossils occur in unit 16. Units 15 and 16 suggest predominantly low-energy environments and gradual increase of salinity as deposition progressed.

FIGURE 35.—Brecciated "crust" that caps unit 5, Stop 6b. Plane-polarized light, X20.

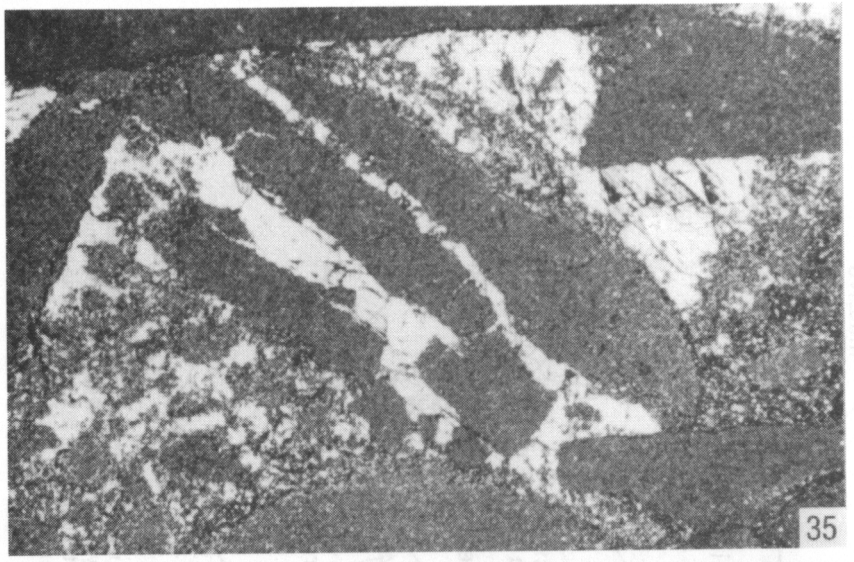

FIGURE 36.—Bioturbated micritic/biomicritic to pelmicritic wackestone/packstone with diverse paleobiota. Unit 7, Stop 6b. Plane-polarized light, X20.

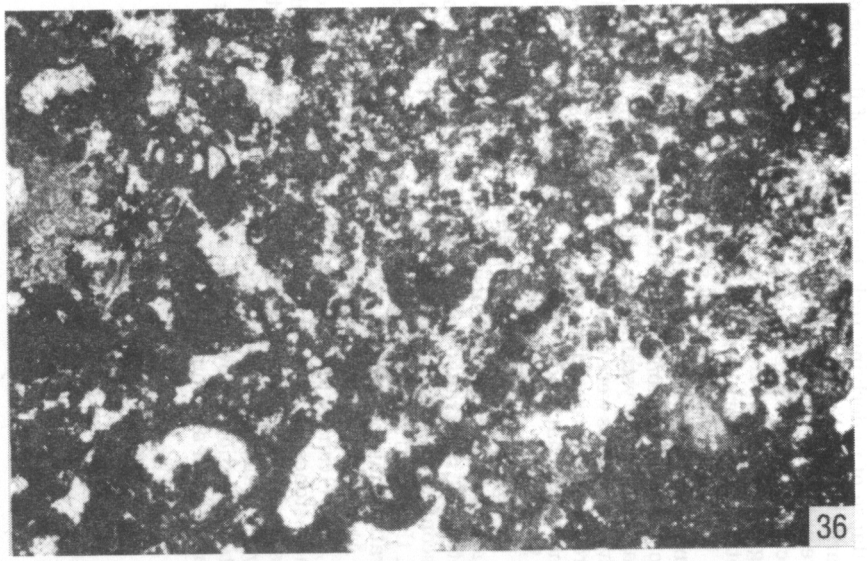

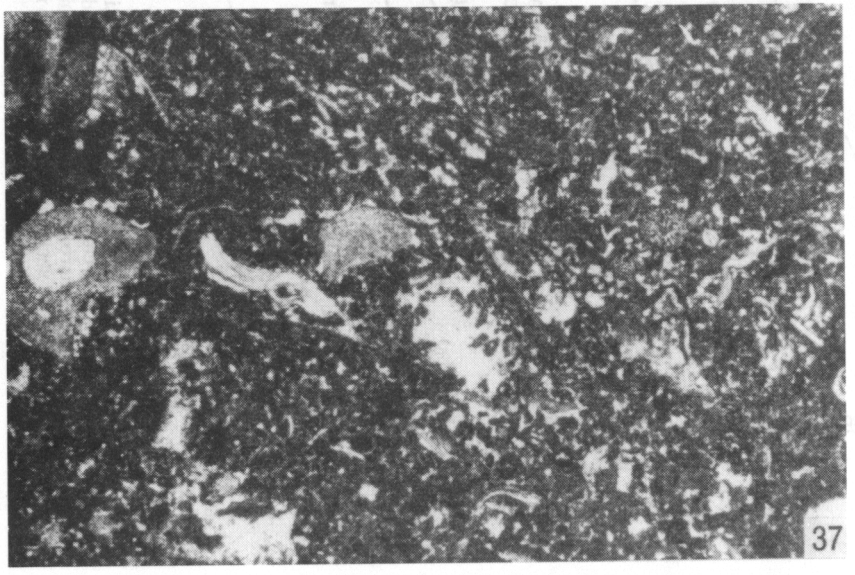

FIGURE 37.—Bioturbated biomicritic wackestone/packstone and biopelsparite that contains relatively diverse paleobiota. Unit 11, Stop 6b. Plane-polarized light, X20.

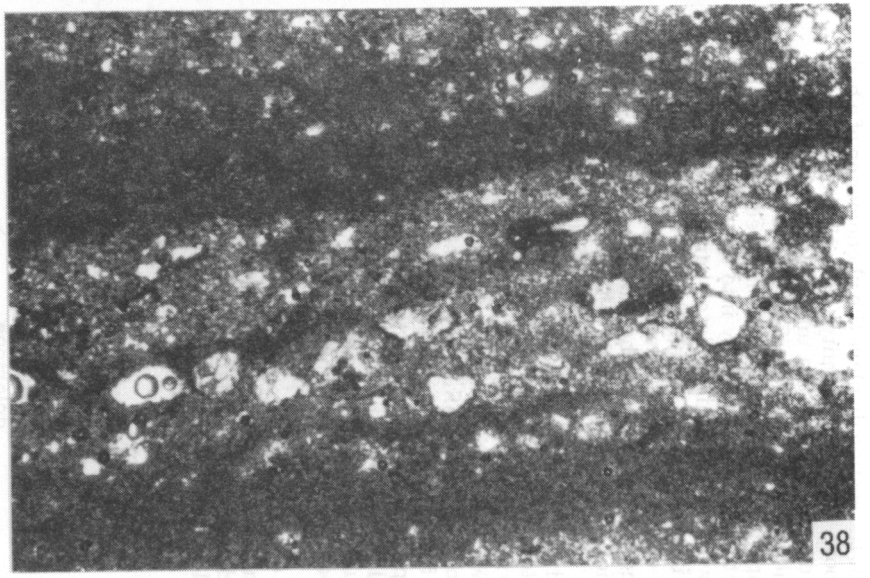

FIGURE 38.—Stromatolitic calcitic dolostone showing alternating layers of micrite and microsparite. Coarse crystals are fillings of minute burrows (extending downward from overlying unit) or salt-crystal pseudomorphs; some may be replaced skeletal fragments. Unit 13, Stop 6b. Plane-polarized light, X20.

At Stop 6c the section displays the phenomenon of a bed that lies above the disconformity (unit 15) bending conspicuously downward into the underlying rocks without becoming noticeably fractured (fig. 39). The downward projection apparently was produced when beds beneath the disconformity collapsed, probably into an unfilled cavern associated with disconformity-related karstification. Lack of fractures in unit 15 suggests that the bed was not lithified at the time of collapse, and thus flowed into the collapse feature rather than fracturing and falling into the developing depression (Hattin and Swain, 1990a, 1990b). Desiccation cracks mark the bottom of unit 15 in the collapse feature, and are supporting evidence that the unit was still soft and water rich at the time of downward movement. At the collapse feature, the brecciated upper part of unit 5 was dragged downward during failure of the underlying rock. However, occurrence of loaflike syneresis-cracked cobbles within unit 5 suggests that part of that unit also may have been incompletely lithified at the time of collapse.

At the collapse feature, unit 15 is overlain by a massive, highly bioturbated bed of biomicritic packstone that contains local patches of wackestone and grainstone as well as colonies of the compound phaceloid coral *Acrocyathus proliferus*. Clearly, this unit was deposited in the most nearly normal marine environment of the unit 13-unit 16 interval and signifies still higher energy conditions than units 14 and 15. At Stop 6c, unit 16 was also affected by the collapse of underlying rock, but instead of flowing downward the rock became highly brecciated (fig. 39). Thus, we are presented with the enigma of a buried, older carbonate-rock unit (unit 15) remaining nonlithified after the overlying bed (unit 16) had become lithified. Stratigraphic and petrographic work continues on this rather exotic question.

Unit 16 is succeeded by a noncalcareous shale parting (unit 17) that contains a lens of diversely fossiliferous biomicritic packstone/biosparite. Unit 16 is overlain by a massive microcrystalline calcitic dolostone (unit 18) in which no fossils were recorded. The latter unit may indicate a return to restricted marine conditions that presaged the emergence that produced the younger disconformity visible at Stop 6a.

Units 19 through 24 are an alternating sequence of silty shales and fossiliferous limestones and chert that form a noticeable reentrant on the cliff face. Although the younger disconformity detected at Stop 6a is not easily traced to Stop 6c, the reentrant at Stop 6c is at approximately the same stratigraphic position.

Above the reentrant, the uppermost sampled beds (units 25, 26, 27) consist predominantly of bioturbated biomicritic wackestones/packstones and a small amount of fossiliferous grainstone (in unit 26); they contain an abundant and diverse paleobiota. Textures, structures, and fossils indicate deposition in low to moderately high energy normal-marine shelf environments.

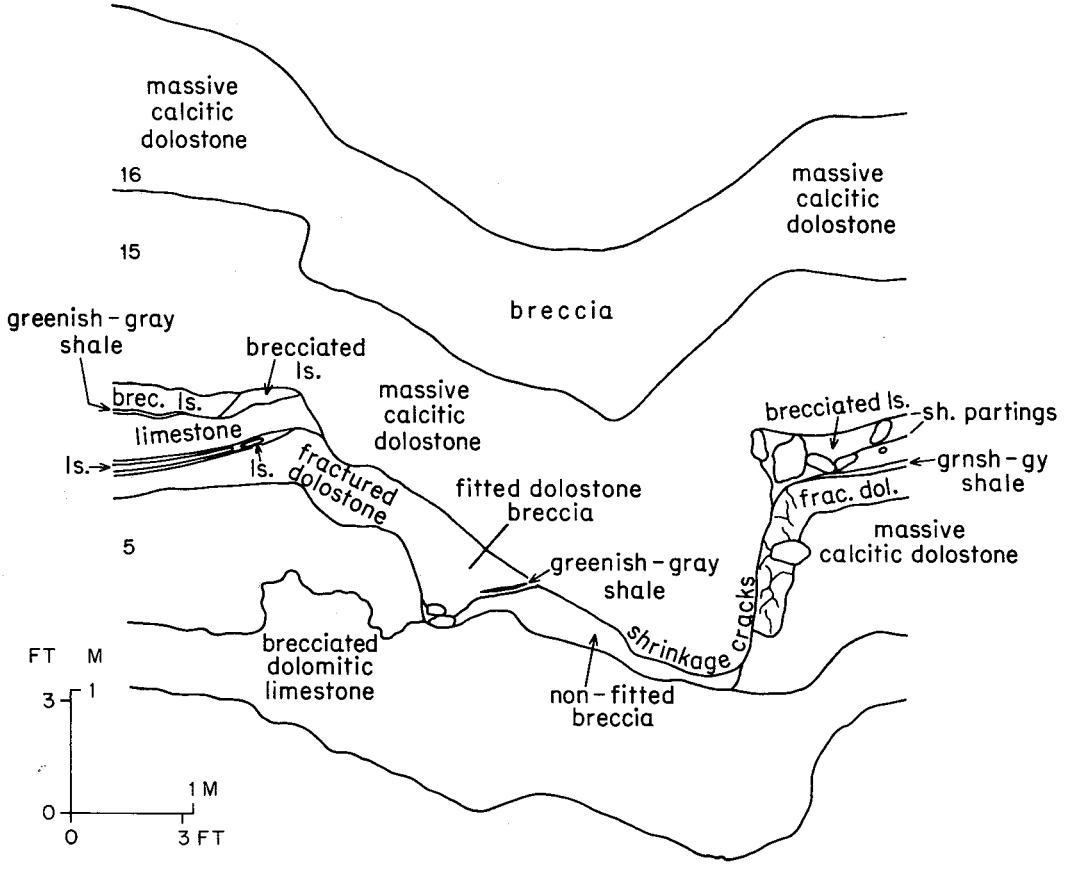

FIGURE 39.—Cross section of collapse-induced deformation in units 15 and 16 in St. Louis Limestone at Stop 6c. Unit 5 was also affected greatly by collapse of the underlying rock. Note that unit 16 became brecciated over the collapse feature, whereas underlying unit 15 did not, suggesting that unit 15 was still unlithified. Cross section is based on 12 sections measured at 2-foot intervals by D. E. Hattin and S. H. Swain in 1989 and 1990.

The stratigraphic succession at Stop 6 is cut by two disconformities. The older one is clearly recognizable throughout McCormick's Creek canyon and has been recognized also in Putnam County, Indiana, some 29 miles (46 km) to the north-northwest, where breccia-filled paleocaverns are also preserved beneath the break. Additional study in progress will determine whether this and other disconformities in the St. Louis are products of local tectonically controlled phenomena, or more widespread features that were produced by extrabasinal factors.

Ettensohn and others (1988) note that intraformational soil profiles developed on carbonate rocks are everywhere thin and immature, whereas interformational profiles are mature and represent much longer times of subaerial exposure. The large-scale karstification evident beneath the older disconformity at Stop 6 suggests that this break is of the latter type, and separates rocks that are best assigned to two different formations.

Climate profoundly affects the kinds of textural, compositional, and structural changes that occur in carbonate sediments that are exposed to subaerial weathering. Characteristic features of rocks weathered under arid, semi-arid, and wet climatic conditions are summarized and illustrated by Choquette and James (1988), who note that calcrete development is a characteristic alteration product in semi-arid regions, where intensive evaporation occurs after rainfalls. In contrast, karstic phenomena, including sinkholes, caves, subsurface dissolution-collapse breccia, and terra rossa, are characteristic products of carbonate-sediment alteration in warm, wet climates. Ettensohn and others (1988) invoke alternately moist and semi-arid conditions to explain development of caliche in the St. Louis Limestone of the Appalachian Basin of eastern Kentucky. Such conditions are suggested also by the calcretes that are preserved in the Ste. Genevieve Limestone of Stops 1 and 4 of this guidebook, and the St. Louis Limestone of Stop 5. The extensive development of karstic phenomena beneath the older of the two disconformities at Stop 6, including apparent remnants of terra rossa and gley soils, sinkholes, caverns, and intraformational autobreccias, are evidence of at least temporarily wet climatic conditions. Occurrence of emergence surfaces associated with calcrete and an emergence surface associated with major karstic phenomena shows that significant climatic fluctuations occurred during deposition of the St. Louis-Ste. Genevieve section in the southwestern Indiana part of the Valmeyeran carbonate shelf.

ACKNOWLEDGMENTS

We extend special thanks to Ralph Hunter, who discovered the eolianite facies in the Ste. Genevieve Limestone, and who gave help and encouragement during our work on Ste. Genevieve exposures in the Corydon area. Thanks also to Donald Carr, who assisted us with field work on the oolitic shoal at Stop 3 (Orleans). Patricia Merkley, Charles Zuppann, Clay Harris, and Karl Leonard contributed extensively to interpretation of depositional history of the Ste. Genevieve, and their help is gratefully acknowledged. Frank Ettensohn accompanied us to Stops 1, 2, and 6, and Robin Bathurst accompanied us to Stops 1, 3, 4, 5, and 6. Both of these friends made numerous suggestions that helped us refine our interpretation of emergence phenomena, and we thank them for giving freely of their extensive knowledge. Carl Rexroad assisted in the identification of conodonts in the section exposed at Stop 6, and he and John Droste gave freely of their knowledge of Valmeyeran lithostratigraphic classification. Very special thanks are extended to Sandra H. Swain, daughter of Donald E. Hattin, for recognizing and calling to Hattin's attention the disconformities and buried paleokarstic features in McCormick's Creek State Park. She also assisted extensively with measurement of sections at Stop 6 and in picking conodonts from samples collected at the park. Thanks, Sandy!

REFERENCES CITED

Bagby, B. L., 1989, Paleoenvironmental and diagenetic analysis of the St. Louis Limestone: M.S. thesis (unpub.), Indiana University, 71 p.

Ball, M. M., 1967, Carbonate sand bodies of Florida and the Bahamas: Journal of Sedimentary Petrology, v. 37, p. 556-591.

Beede, J. W., 1911, The cycle of subterranean drainage as illustrated in the Bloomington, Ind., quadrangle: Indiana Academy of Science, Proceedings, 1910, p. 81-103.

Brown, M. A., 1987, Regional lithofacies and depositional environments of the Salem Limestone (Valmeyeran, Mississippian), south-central Indiana, *in* Thompson, T. A., ed., Architectural elements and paleoecology of carbonate shoal and intershoal deposits in the Salem Limestone (Mississippian) in south-central Indiana: Indiana Geological Survey Guidebook 14, 75 p.

Brown, M. A., Archer, A. W., and Kvale, E. P., 1990, Neap-spring tidal cyclicity in laminated carbonate channel-fill deposits and its implications: Salem Limestone (Mississippian) south-central Indiana, U.S.A.: Journal of Sedimentary Petrology, v. 60, p. 152-159.

Carr, D. D., 1973, Geometry and origin of oolite bodies in the Ste. Genevieve Limestone (Mississippian) in the Illinois Basin: Indiana Geological Survey Bulletin 48, 81 p.

Choquette, P. W., and James, N. P., 1988, Introduction, *in* James N. P., and Choquette, P. W., eds., Paleokarst: New York, Springer-Verlag, p. 1-21.

Choquette, P. W., and Steinen, R. P., 1980, Mississippian non-supratidal dolomite, Ste. Genevieve Limestone, Illinois Basin: evidence for mixed-water dolomitization: Society of Economic Paleontologists and Mineralogists Special Publication 28, p. 163-196.

Cluff, R. M., 1984, Carbonate sand shoals in the Middle Mississippian (Valmeyeran) Salem-St. Louis-Ste. Genevieve Limestones, Illinois Basin: *in* Harris, P. M., ed., Carbonate sands, a core workshop: Society of Economic Paleontologists and Mineralogists Core Workshop Notes 5, p. 94-135.

Cluff, R. M., and Lineback, J. A., 1981, Middle Mississippian carbonates of the Illinois Basin: Illinois Geological Society and Illinois State Geological Survey, 87 p.

Coveny, R. M., Jr., Watney, W. L., and Maples, C. G., 1991, Contrasting depositional models for Pennsylvanian black shale discerned from molybdenum abundances: Geology, v. 19, p. 147-150.

Dembecki, Harry, Jr., Meinschein, W. G., and Hattin, D. E., 1976, Possible environmental significance of the predominance of even-carbon number C_{20}-C_{30} n-alkanes: Geochimica et Cosmochimica Acta, v. 40, p. 203-208.

Dodd, J. R., Zuppann, C. W., Harris, C. D., and Leonard, K. W., 1990a, Differential rates of lateral and vertical accretion of an ooid shoal, Ste. Genevieve Limestone, Orleans, Indiana (abs.): Geological Society of America Abstracts with Programs, v. 22, p. 132.

Dodd, J. R., Brown, T. W., Harris, C. D., Leonard, K. W., and Zuppann, C. W., 1990b, Petrology of Mississippian carbonate eolianites and associated facies: Ste. Genevieve Limestone of Indiana (abs.): American Association of Petroleum Geologists Bulletin 74, p. 642-643.

Dodd, J. R., Zuppann, C. W., Harris, C. D., Leonard, K. W., and Brown, T. W., in press, Petrographic method of distinguishing eolian and marine grainstones, Ste. Genevieve Limestone (Mississippian) of Indiana, *in* Keith, B. D., and Zuppann, C. W., eds., Mississippian oolites and Recent analogs: American Association of Petroleum Geologists, Studies in Geology.

Droste, J. B., and Carpenter, G. L., 1990, Subsurface stratigraphy of the Blue River Group (Mississippian) in Indiana: Indiana Geological Survey Bulletin 62, 45 p.

Enos, Paul, 1983, Shelf environment, *in* Scholle, P. A., Bebout, D. C., and Moore, C. H., eds., Carbonate depositional environments: American Association of Petroleum Geologists Memoir 33, p. 268-295.

Esteban, Mateu, and Klappa, C. F., 1983, Subaerial exposure environment, *in* Scholle, P. A., Bebout, D. C., and Moore, C. H., eds., Carbonate depositional environments: American Association of Petroleum Geologists Memoir 33, p. 1-54.

Ettensohn, F. R., Dever, G. R., Jr., and Grow, J. S., 1988, A paleosol interpretation of profiles exhibiting subaerial exposure "crusts" from the Mississippian of the Appalachian Basin, *in* Reinhardt, Juergen, and Sigleo, W. R., Paleosols and weathering through geologic time: principles and applications: Geological Society of America Special Paper 216, p. 49-79.

Hanford, C. R., 1990, Mississippian carbonate eolianites in southwestern Kansas (abs.): American Association of Petroleum Geologists Bulletin 74, p. 669.

Hattin, D. E., and Swain, S. H., 1990a, Valmeyeran emergence and karstification of St. Louis Limestone, Owen County, Indiana (abs.): Geological Society America Abstracts with Programs, v. 22, p. 9.

Hattin, D. E., and Swain, S. H., 1990b, Valmeyeran (Middle Mississippian) emergence and karstification of marine carbonate sediments: evidence within St. Louis Limestone of Owen County, Indiana (abs.): Nottingham, England, 13th International Sedimentological Congress, Abstracts of Posters, p. 98-99.

Hunter, R. E., 1988, Eolianities in the Ste. Genevieve Limestone (Mississippian) of Southern Indiana (abs.): Society of Economic Paleontologists and Mineralogists Midyear Meeting Abstracts, v. 5, p. 26-27.

Hunter, R. E., 1989, Eolianites in the Ste. Genevieve Limestone of southern Indiana: *in* Field Trip Guidebook, Eastern Section American Association of Petroleum Geologists, p. 1-19.

Jorgensen, D. B., and Carr, D. D., 1973, Influence of cyclic deposition, structural features, and hydrologic controls on evaporite deposits in the St. Louis Limestone in southwestern Indiana, *in* Proceedings of the 8th Forum on the Geology of Industrial Minerals: Iowa Geological Survey Public Information Circular 5, p. 43-65.

Kahle, C. F., 1988, Surface and subsurface paleokarst, Silurian Lockport and Peebles Dolomites, western Ohio, *in* James, N. P., and Choquette, P. W., eds., Paleokarst: New York, Springer-Verlag, p. 229-255.

Keller, S. J., and Becker, L. E., 1980, Subsurface stratigraphy and oil fields in the Salem Limestone and associated rocks in Indiana: Indiana Geological Survey Occasional Paper 30, 63 p.

Knewtson, S. L., and Hubert, J. F., 1969, Dispersal patterns and diagenesis of oolitic calcarenites in the Ste. Genevieve Limestone (Mississippian), Missouri: Journal of Sedimentary Petrology, v. 39, p. 954-968.

Leibold, A. W., 1982, Stratigraphy, petrography, and depositional environment of the Bryantsville Breccia (Meramecian) of south-central Indiana: A.M. thesis (unpub.), Indiana University, 171 p.

Loope, D. B., 1986, Pennsylvanian eolian limestones, Paradox Basin, U.S.A. (abs.): 12th International Sedimentological Congress, Abstracts Volume, p. 189-190.

Loope, D. B., and Haverland, Z. E., 1988, Giant desiccation fissures filled with calcareous eolian sand, Hermosa Formation (Pennsylvanian), southeastern Utah: Sedimentary Geology, v. 56, p. 403-413.

Malott, C. A., 1922, The physiography of Indiana, *in* Logan, W. N., Cumings, E. R., Malott, C. A., Visher, S. S., Tucker, W. M., and Reeves, J. R., Handbook of Indiana geology: Indiana Department of Conservation, Division of Geology, Publication 21, p. 62-276.

Malott, C. A., 1952, Stratigraphy of the Ste. Genevieve and Chester formations of southern Indiana: Ann Arbor, Edwards Letter Shop, 105 p.

Merkley, P. A., 1991, Origin and distribution of carbonate eolianites in the Ste. Genevieve Limestone (Mississippian) of southern Indiana and northeastern Kentucky: M.S. thesis (unpub.), Indiana University, 147 p.

Nellist, W. E., Perucca, M. A., and Hattin, D. E., 1985, Faunal analysis of a shallow-water organic-rich black shale from the St. Louis Limestone (Valmeyeran) of south-central Indiana (abs.): Geological Society of America Abstracts with Programs, v. 17, p. 320.

Perrin, S. E., 1986, Depositional environments and subsurface geometry of oolitic grainstones in the Ste. Genevieve Limestone (Valmeyeran), Owensville North Field, Gibson County, Indiana: A.M. thesis (unpub.), Indiana University, 172 p.

Ray, W. L., 1986, The origin and distribution of oolite zones in the Ste. Genevieve Limestone (Valmeyeran), Posey County, Indiana: M.S. thesis (unpub.), Indiana University, 94 p.

Rexroad, C. B., Woodson, F. J., and Knox, L. W., 1990, Revised boundary between the St. Louis and Ste. Genevieve limestones (Middle Mississippian) on outcrop in Indiana (abs.): Geological Society of America Abstracts with Programs, v. 22, p. 31.

Rice, J. A., and Loope, D. B., 1987, Pennsylvanian eolian limestones, western Grand Canyon and southern Nevada (abs.): Geological Society of America Abstracts with Programs, v. 19, p. 818.

Rice, J. A., and Loope, D. B., 1991, Wind-reworked carbonates, Permo-Pennsylvanian of Arizona and Nevada: Geological Society of America Bulletin 103, p. 254-267.

Sarg, J. F., 1988, Carbonate sequence stratigraphy, *in* Wilgus, C. K., Hastings, B. K., Posamentier, Henry, VanWagoner, John, Ross, C. A., and Kendall, C. G. St. C., eds., 1988, Sea-level changes: an integrated approach: Society of Economic Paleontologists and Mineralogists Special Publication 42, p. 155-181.

Shaver, R. H., and many others, 1986, Compendium of Paleozoic rock-unit stratigraphy in Indiana - a revision: Indiana Geological Survey Bulletin 59, 203 p.

Shinn, E. A., 1983, Tidal flat environment, *in* Scholle, P. A., Bebout, D. G., and Moore, C. H., eds., Carbonate depositional environments: American Association of Petroleum Geologists Memoir 33, p. 172-210.

Thornbury, W. D., 1965, Regional geomorphology of the United States: New York, John Wiley, 609 p.

Wilson, J. L., 1975, Carbonate facies in geologic history: New York, Springer-Verlag, 471 p.

Woodson, F. J., 1982, Uppermost St. Louis Limestone (Mississippian): the Horse Cave Member in Indiana: Indiana Academy of Science Proceedings, v. 91, p. 419-427.

Zinn, L. A., 1983, Subsurface stratigraphy of the Ste. Genevieve Limestone (Meramecian) and relation to underlying Silurian reefs, Greene County, Indiana: Bloomington, Indiana University, A.M. thesis (unpub.), 187 p.

APPENDIX: DESCRIPTIONS OF MEASURED SECTIONS

DESCRIPTION AND ENVIRONMENTAL INTERPRETATION OF MEASURED SECTION AT STOP 1*

(see figure 11)

Ste. Genevieve Limestone (part)	thickness (meters)
R. Grainstone to rudstone, skeletal (echinodermal), cross-bedded (small-scale trough and planar), decreasing grain size upward. HIGH-ENERGY MARINE.	1.0
Q. Grainstone to packstone, oolitic, large skeletal grains, crinoids, brachiopods, and gastropods, medium- to coarse-grained, basal contact sharp. HIGH-ENERGY MARINE.	1.65
P. Mudstone and shale, interbedded, basal contact sharp and irregular. LOW-ENERGY MARINE	0.65
O. Grainstone to mudstone, lower third mudstone to wackestone, silty, burrowed, grades upward to massive oolitic grainstone, pyrite, abundant stylolites. LOW- TO HIGH-ENERGY MARINE	3.2
N. Grainstone, intraclastic conglomerate at base grading upward to evenly laminated, medium- to coarse-grained, well-rounded, highly spherical grains, tightly packed (extensive solution packing), mixed-clast grainstone, minor packstone lenses (calcrete horizons), rhizocretions. EOLIAN	1.2
M. Wackestone, dolomitic, skeletal grains, quartz sand and silt, skeletal content increases upward, breccia at top, basal contact transitional. LOW-ENERGY MARINE	2.85
L. Mudstone, silty, dolomitic, recessive weathering, brachiopods, pyrite, burrowed, intercrystalline porosity. LOW-ENERGY MARINE	1.4
I. Grainstone, intraclastic conglomerate at base, evenly and thinly cross-laminated (large-scale trough cross-bed sets), medium- to coarse-grained mixed-clast grainstone, abundant quartz sand and silt, well-rounded, highly spherical grains, tightly packed (extensive solution packing), inverse grading in some laminae, upper surface burrowed in places, ripple marks locally. EOLIAN	6.0
H. Grainstone to packstone, chert nodules and layers and clay partings at base, cross-bedded in part, medium-grained, upper part brecciated, possible rhizocretions, thickness variable. MODERATE- TO HIGH-ENERGY MARINE	0.65
G. Grainstone to packstone, laminated, abundant chert nodules and shale lenses, possible stromatolites. LOW-ENERGY MARINE	0.5
F. Grainstone, coarse conglomerate at base, grades upward to evenly and thinly cross-laminated mixed-clast grainstone, abundant quartz sand and silt, medium- to coarse-grained, well-rounded, highly spherical grains, tightly packed, rhizocretions, thins away from center of exposure. EOLIAN	2.1
E. Grainstone to packstone, massive, medium- to coarse-grained, oolitic, contains large corals, mud content decreases upward, upper surface locally brecciated. HIGH-ENERGY MARINE	2.7
D. Mudstone to wackestone, dolomitic. LOW-ENERGY MARINE	0.4
C2. Mudstone to packstone, dolomitic, scattered pods of oolitic grainstone at low areas in irregular base, base scoured. LOW- TO MODERATE-ENERGY MARINE	1.0
C1. Mudstone to packstone, dolomitic, base covered. LOW- TO MODERATE-ENERGY MARINE	1.2
Total thickness of measured section	26.5 m

*Section measured by P. A. Merkley, J. R. Dodd, C. D. Harris, K. W. Leonard, and C. W. Zuppann in 1989.

DESCRIPTION AND ENVIRONMENTAL INTERPRETATION OF MEASURED SECTION AT STOP 2*

(see figure 12)

Ste. Genevieve Limestone (part)	thickness (meters)
R. Grainstone to rudstone, skeletal (echinoderms and bryozoans), cross-bedded (herringbone?), basal contact sharp and irregular. HIGH-ENERGY MARINE	0.8
Q. Grainstone, oolitic, well-sorted, loosely packed, medium-to coarse-grained, isopachous rim cement, basal contact sharp and regular. HIGH-ENERGY MARINE.	0.95
P. Packstone to wackestone, skeletal, slightly washed in places, massive. LOW-ENERGY MARINE	0.25
O. Grainstone to wackestone, fine- to medium-grained, numerous stylolites, skeletal grainstone, loosely packed, thick isopachous rim cement, micrite partially dolomitized, oolitic grainstone in upper part. LOW-TO HIGH-ENERGY MARINE.	3.0
N. Grainstone, intraclastic conglomerate at base grading upward to evenly cross-laminated, fine- to medium-grained mixed-clast grainstone, well-rounded, highly spherical grains, tightly packed (extensive solution packing), quartz silt, large pyrite crystals, rhizocretions. EOLIAN	1.6
M. Wackestone to mudstone, dolomitic, pellets and skeletal grains, quartz silt, fine- to medium-grained, abundant large-amplitude stylolites. LOW-ENERGY MARINE.	2.4
L. Packstone to wackestone, quartz silt, fine-grained abundant clay partings, brachiopods, colonial corals, echinoderms, recessive weathering. LOW-ENERGY MARINE	1.55
K. Grainstone, thinly and evenly cross-laminated, mixed-clast, medium- to coarse-	

grained, well-sorted within laminae, well-rounded and highly spherical grains, tightly packed (extensive solution packing), abundant quartz silt, rhizocretions. EOLIAN	0.4
J. Shale, calcareous, molluscan fossils. LOW-ENERGY MARINE	0.25
I. Grainstone, intraclastic conglomerate at base, grades upward to evenly and thinly cross-laminated, fine- to medium-grained, mixed-clast grainstone, well-rounded and highly spherical grains, contains calcrete and rhizocretions, large pyrite crystals, upper surface burrowed in places. EOLIAN	1.3
H. Wackestone, skeletal, fine- to medium-grained, wavy laminae with clay partings at base, calcite-filled burrows, rhizoliths, grades upward into a fine- to medium-grained, poorly washed skeletal and peloidal grainstone, thickness variable. LOW- TO MODERATE-ENERGY MARINE	1.5
G. Packstone to mudstone, thinly and irregularly laminated (stromatolitic?), birdseye texture locally, fluoritic and chert layers, thickness variable. LOW-ENERGY MARINE	0.35
F. Grainstone, intraclastic conglomerate at base, grades upward to evenly and thinly cross-laminated mixed-clast grainstone, medium- to coarse-grained, well-rounded highly spherical grains, tightly packed (extensive solution packing), abundant quartz silt. EOLIAN	1.85
E. Grainstone, massive, medium-grained, oolitic, also skeletal lenses, well sorted, moderate packing, isopachous rim cement, large intraclasts in upper part, contains large horn and colonial corals. HIGH-ENERGY MARINE	3.0
D. Wackestone to mudstone, dolomitic, massive, highly fractured, thinly laminated in places. LOW-ENERGY MARINE	0.3
C2. Wackestone to mudstone, dolomitic, scattered pods of oolitic and skeletal grainstone at low areas along irregular base, scattered pyrite crystals, base scoured, thickness variable. LOW-ENERGY MARINE	1.6
C1. Wackestone to mudstone, dolomitic, large intraclasts at base, evenly laminated at base (stromatolitic?), numerous stylolites. LOW-ENERGY MARINE	0.7
B. Rudstone to grainstone, numerous gastropods, thickness variable due to irregular upper surface. HIGH-ENERGY MARINE.	0.3
A. Grainstone to packstone with some rudstone, skeletal, fine- to medium-grained, poorly sorted and rounded, abundant laminated chert layers and nodules, large fenestrate bryozoans, large-scale stylolites, base covered. MODERATE-ENERGY MARINE.	2.7
Total thickness of measured section	24.8 m

*Section measured by P. A. Merkley in 1990 and slightly modified by J. R. Dodd in 1991.

DESCRIPTION AND ENVIRONMENTAL INTERPRETATION OF MEASURED SECTION AT STOP 3*
(see figure 13)

Ste. Genevieve Limestone	thickness (meters)
6. ** Grainstone, oolitic, fine- to coarse-grained, gastropods and echinoderms, dolomite-filled burrows, isopachous rim cement, top not exposed. HIGH-ENERGY MARINE	0.3
5. **Wackestone to mudstone, scattered packstone stringers, very dense, breaks with conchoidal fracture, scattered gastropods, brachiopods, echinoderms, bryozoans, sponge spicules, peloids, thin dolomitic horizons, stylolites common, abundant burrows at top. LOW-ENERGY MARINE	4.25
4. **Grainstone to wackestone, quartz sand common, fenestrate bryozoans, ostracodes, gastropods, brachiopods, sponge spicules, peloids, common stylolites, grains coarsen upward. VARIABLE-ENERGY MARINE.	0.7
3. **Grainstone to wackestone, oolitic at top, skeletal in part, echinoderms, brachiopods, gastropods, peloids, fine- to medium-grained, mud content decreases upward, upper portion brecciated (probably exposure surface). VARIABLE-ENERGY MARINE	0.5
2. Grainstone, oolitic, skeletal grains (especially near top), massive, cross-bedding visible on weathered surfaces, mostly medium-grained, some coarse-grained in upper part, echinoderms, gastropods, brachiopods, corals, bryozoans, large (up to 10 cm) intraclasts in upper part, isopachous rim cement in upper part, loose packing toward top, tighter packing near base, stylolites common, very large stylolite 4.8 m above base. HIGH-ENERGY MARINE.	8.1
1. Wackestone to mudstone, partially dolomitized, neomorphosed, scattered fossils (brachiopods, bryozoans, gastropods), peloids, burrowed, upper surface irregularly hummocky, possibly bored, contains fractures filled with sediment from overlying unit, upper contact stylolitic in part, base not exposed. LOW-ENERGY MARINE	1.0
Total thickness of measured section	14.85 m

*Section measured by J. R. Dodd, C. W. Zuppann, C. D. Harris, and K. W. Leonard in 1989.
**Unit 6 is unit 4 in figure 13. Units 3, 4, and 5 included in unit 3 in figure 13.

DESCRIPTION OF MEASURED SECTION AT STOP 4*
(see figure 14)

Ste. Genevieve Limestone (upper part)	thickness (meters)
15. Limestone, predominantly micritic, classic sparry-calcite-filled birdseye vugs; extensively brecciated, displaced blocks of birdseye limestone as large as 0.55 m wide and 0.24 m thick. Partly intrasparrudite, with very fine sand- to fine-pebble-sized clasts composed of intraclastic wackestone and many rounded, sand-sized clasts consisting of micrite or micrite-coated skeletal grains. Irregular, crinkly micrite as grain coatings and thin irregular stringers (calcrete), contains elongate sparry-calcite-filled tubules (rhizomorphs), accompanied locally by patches of rock with alveolar structure. Brecciated rock cemented by sparry calcite; some original interstices in breccia filled with intrasparite. Sparse, rounded clasts of oolitic intrasparite reworked from unit 14 partly rimmed by crinkly micrite (calcrete). Unit contains sparse silt- and very fine sand-sized quartz grains, some in reworked clasts	0.49
14. Limestone, silty to coarsely sandy oolitic intrasparite; laminated, with well-sorted silt/very fine sand laminae alternating with poorly sorted very fine to coarse sand laminae; coated grains common, with bryozoan, echinoderm, ostracode, and mollusc remains as cores; echinoderm debris common; ostracodes, calcispheres, brachiopod fragments sparse. Irregular stringers of micritized rock (calcrete) scattered throughout, some contain tubular structures (rhizomorphs) filled with sparry calcite	0.31
13. Limestone, silty to coarsely sandy oosparite; laminated, with well-sorted silt/very fine sand laminae alternating with poorly sorted very fine to coarse sand laminae; ooids and coated skeletal grains predominate throughout; peloids and rounded intraclasts common; composite grains sparse; skeletal grains are echinoderm debris, ostracodes, and bryozoan fragments; about 1 percent of rock is angular grains of quartz silt and very fine sand.	0.14
12. Clay parting, weathered, with very thin local lenses of very fine-grained skeletal packstone; ostracodes common	0.009
11. Limestone, mostly very fine- to medium-grained oolitic biomicritic wackestone with local patches of fossiliferous oolitic grainstone; bioturbated fabric; ooids and echinoderm debris abundant; ostracodes, calcispheres, and mollusc fragments common; bryozoan fragments sparse; forams rare. Irregularly elongated patches of sparry calcite common. Upper 0.045 m mostly biomicritic wackestone with patches of oomicritic packstone/grainstone; bioturbated fabric; irregularly brecciated into sand- and small-pebble-sized clasts; peloids and ooids/coated grains abundant; echinoderm debris, calcispheres, and ostracodes common; bryozoan and brachiopod debris rare. Uppermost part of bed has fenestral fabric	0.52
10. Limestone, very fine- to coarse-grained biomicritic packstone/wackestone, with local patches of grainstone; bioturbated fabric; echinoderm debris abundant; mollusc fragments, brachiopod fragments, bryozoan fragments, ostracodes, and calcispheres common; peloids sparse	0.14
9. Shale parting, weathered	0.006
8. Limestone, lower part mostly biosparitic grainstone with patches of biomicritic wackestone; echinoderm debris abundant; pellets, coated grains, micritized skeletal grains and intraclasts common to abundant; brachiopod fragments, bryozoan fragments, calcispheres, and forams common; recrystallized mollusc fragments and ostracodes sparse; locally bioturbated fabric. Upper part of unit very fine- to coarse-grained fossiliferous oosparite. Ooids predominate, mostly with skeletal nuclei; echinoderm debris abundant	2.00
7. Limestone, biomicritic packstone, locally grainstone; bioturbated fabric; echinoderm debris, peloids, and coated grains abundant; ostracodes, brachiopod fragments, fenestellid bryozoan fragments, and forams common; gastropods rare; intraclasts sparse. Microstylolitization has created local zones and pods of breccia	0.80
6. Clay parting, calcareous, gritty	0.006-0.009
5. Dolomitic limestone, very fine- to coarse-grained biomicritic wackestone, locally packstone; bioturbated fabric; echinoderm debris and brachiopods common, corals sparse	1.83
4. Limestone, very fine- to very coarse-grained oolitic biosparite; echinoderm debris abundant; bryozoan fragments, gastropods, ostracodes, forams, and brachiopod fragments common	0.18
3. Limestone, very fine- to coarse-grained fossiliferous oosparite; echinoderm debris abundant; ostracodes, forams, and gastropods common. Faint horizontal laminations	0.53
2. Clay parting, calcareous	0.015
1. Limestone, very fine- to medium-grained fossiliferous oosparite; echinoderm debris and intraclasts common; ostracodes and forams sparse; ooids manifest wide variety of invertebrate skeletal nuclei. Faint cross-laminations in part; centimeter-scale burrows in uppermost part	0.97
Total thickness of measured section	7.95 m

*Section measured by J. R. Dodd and D. E. Hattin in 1991.

DESCRIPTION OF MEASURED SECTION AT STOP 5*
(see figure 21)

	thickness (meters)
St. Louis Limestone (lower part)	
21. Dolomitic limestone, micritic mudstone, thinly bedded to laminated, possible ripple marks in lower 0.06 m and approximately 0.23 m above base. No fossils detected ..	0.26
20. Organic-rich shale, grayish-black, very thinly laminated, fissile, composed mainly of wisps, blebs, and other scraps of orange-red organic matter. Very fine sand- and silt-sized quartz grains scattered throughout, locally concentrated in laminae or burrowlike structures. Sparse fish-bone fragments	0.034
19. Limestone, biomicritic packstone, locally wackestone, massive, thoroughly bioturbated; local mud cracks, scattered quartz silt and very fine sand. Ostracodes abundant; *Chondrites* and brachiopod fragments common; *Spirorbis* sparse	0.024
18. Shale, grayish-brown, noncalcareous, very thinly laminated, very slightly silty	0.001
17. Dolomitic limestone, micritic mudstone, massive, upper surface with mud cracks, massive, top part locally intraclastic; very fine sand- and silt-sized quartz grains common; ostracodes and calcispheres very sparse	0.03
16. Calcitic dolomite/dolomitic limestone, micritic mudstone, tightly cemented, brecciated, with millimeter-scale tubular structures filled partially with calcite; in part coarsely brecciated and cemented by blocky crystals of calcite. Rock extends as fingers into unit 15 below	0.012-0.067
15. Limestone, micritic mudstone, all more or less laminated—poorly in basal third, better in central third, well-laminated in upper third; some laminations crinkly to slightly mounded; intraclasts sparse in thin, laminar zones; birdseye structure common, especially in upper part; large calcite-filled vugs in upper half	0.27-0.28
14. Dolomitic limestone and calcitic dolomite, micritic mudstone, all more or less thinly laminated, lighter colored laminae characterized by minute patches of microsparite; locally cross-laminated; small scour structure 0.11 m deep 0.58 m above base. Laminations bundled. Ostracodes and millimeter-scale burrow structures sparse	1.06
13. Limestone, biomicritic packstone/wackestone with patchy areas of mudstone, massive, strongly bioturbated texture, in part pelleted, with sparse intraclasts. Lower 5.5 cm contains small patches of calcite. Ostracodes abundant; forams sparse	0.12-0.22
12. Limestone, micritic mudstone, laminated, small stromatolitic mound at base; laminae deformed around stromatolite; lower half of unit locally truncated by upper half. Scattered ostracodes occur on some bedding planes	0.09-0.12
11. Limestone, fossiliferous intraclastic oomicritic packstone, local areas of grainstone; very fine to very coarse grained; basal 0.05 m laminated, abundant *Chondrites* in upper part; remainder of unit mainly massive, bioturbated, with faintly laminated zone very rich in *Chondrites* near center; pebble-sized intraclasts at top. Ostracodes common; brachiopods, echinoderm debris, and forams sparse; profusion of calcitic branching structures on bottom of bedding plane 0.018 m above base	0.17
10. Shale, dark-yellowish-brown, slightly silty, calcareous, very thinly laminated; micritic lamina near base	0.052
9. Limestone, pelletiferous biomicritic packstone, patches of sparry calcite scattered throughout; bioturbated texture; ostracodes, calcispheres, and echinoderm debris abundant; forams sparse; scattered grains of quartz silt and very fine-grained sand. Small digitate stromatolites common near center of bed; oncolites common near top of bed	0.24
8. Limestone, micritic mudstone, laminated, stromatolitic. Lower half with lenticular structures draped by discontinuous partings of papery shale. Upper half contains large stromatolitic mounds that are separated and overlain by horizontally laminated limestone containing abundant *Chondrites*. Top of unit undulatory, tops of larger mounds protrude above general surface	0.19-0.25
7. Limestone, micritic mudstone, laminated, stromatolitic, laminae crinkly; locally contorted to overturned; alternate laminae darkened by iron oxide; top of bed marked by small mounds, the tops of which are locally disrupted and brecciated. Sparse grains of quartz silt	0.012-0.048
6. Shale, medium-greenish-gray, iron-stained; middle and upper parts contain very thin small lenses of dolomitic intramicrudite.	0.012-0.043
5. Limestone, fossiliferous pelletal intrasparrudite; intraclasts of very fine sand- to pebble-sized micrite with birdseye fabric; coarser intraclasts concentrated in zones centered 0.41 and 0.69 m above base; unit manifests overall coarsening upward; ostracodes and forams common; mollusc fragments sparse	0.83
4. Shale, olive-gray, slightly silty, calcareous; 0.083-0.19 local lens of very fossiliferous intramicritic packstone; small local patches of grainstone	0.083-0.19
3. Limestone, fossiliferous pelmicritic packstone, massive, apparently bioturbated; local small irregular patches of pelsparite; forams, brachiopods, corals, ostracodes, and echinoderm debris common; calcispheres sparse; micritic intraclasts common in thin interval lying 0.06 m below top	0.28
2. Shale, greenish-gray, noncalcareous	0.05-0.18
Total thickness of exposed St. Louis	4.10 m
Salem Limestone (top bed only)	
1. Limestone, pelletiferous biomicritic packstone; calcispheres and mollusc debris abundant; echinoderm debris common, brachiopod fragments and ostracodes sparse	1.07
Total thickness of measured section	5.17 m

*Section measured by Donald E.Hattin in 1989.

DESCRIPTION OF MEASURED SECTION AT STOP 6a
(see figure 27)

St. Louis Limestone (part)	thickness (meters)
Disconformity, with local relief as great as 2.8 m.	
22. Carbonate-rock breccia; clasts of limestone and calcitic dolomite; set in poorly sorted carbonate matrix	1.4-3.1
21. Calcitic dolomite and dolomitic limestone, 0.29-0.35 massive micritic/microsparitic mudstone, grades upward through (a) crudely banded zone of tightly cemented micrite, (b) partially brecciated rock with abundant alveolar structure, and (c) brecciated rock cemented by microsparite and blocky spar calcite. Forams sparse	0.29-0.35
20. Shale parting, noncalcareous, grayish-brown, laminated slightly silty	0.003
19. Dolomitic limestone, mostly massive micritic to microsparitic mudstone, scattered dolorhombs; minute sparry-calcite-filled burrow-like structures common; basal 0.06 m riddled with *Chondrites*	0.34
18. Dolostone, mudstone, with thin crinkly "laminations" formed by microstylolites.	0.024
17. Shale parting, noncalcareous, laminated, grayish-brown, brittle	0.02
16. Limestone, massive, micritic mudstone, biomicritic wackestone, and biomicritic packstone with bioturbated texture. Fine sand- to silt-sized skeletal debris of indeterminate origin. Discrete burrow structures filled with blocky sparry calcite or micrite, some filled with finely crystalline quartz	0.53
15. Shale parting, noncalcareous, grayish-brown with dark-green staining, clayey, brittle.	0.003
14. Dolomitic limestone, massive, micritic mudstone with bioturbated texture; part of rock ordinary micrite, remainder with scattered grains of quartz silt. *Chondrites* common locally in bed, filled with pelmicrosparite or biosparite/biomicrosparite; ostracodes sparse, other shelly debris common, including tubular spines (productoid brachiopods?)	0.46
13. Calcitic dolomite/dolomitic limestone, massive, micritic mudstone with fine-pebble micritic lithoclasts set in a micritic matrix that also contains abundant grains of quartz silt and very fine to fine sand. Forms noticeable reentrant	0.55
12. Limestone, massive, brecciated mudstone; large microsparitic clasts contain smaller, darker colored micritic clasts and are set in a matrix of micrite that contains minute micritic clasts and scattered grains of quartz silt and very fine to fine sand	0.21
11. Shale parting, noncalcareous, grayish-brown with dark-green staining, slightly silty clay. Mainly illite with minor quartz and accessory illite/smectite and dolomite	0.006
10. Calcitic dolomite, micritic mudstone, in part with crinkly laminations formed by microstylolites	0.47
9. Shale parting, noncalcareous, grayish-brown, laminated, finely silty	0.006
8. Dolomitic limestone and calcitic dolostone, micritic mudstone, mostly massive, with faint laminations and cross-laminations in upper 0.2 m; uppermost 0.05 m contains partially dolomitized lenses of skeletal grainstone with sharp bases; basal 0.09 m contains sparse laminae of biomicritic to biosparitic wackestone/packstone/grainstone containing ostracodes, brachiopod? fragments, and a few intraclasts that alternate with laminae of mudstone. Local patches of dolomicrosparite. Sparry-calcite-filled burrow structures sparse	0.58
7. Shale parting, noncalcareous, grayish-brown with dark-green staining, laminated, finely silty	0.006
6. Dolomitic limestone; lower 0.15 m micritic mudstone, remainder finely brecciated; breccia clasts are mudstone and range up to fine-pebble size, matrix is lighter colored micrite/microsparite and contains minute crystals of gypsum	0.44
5. Shale parting, noncalcareous, grayish-brown, finely silty	0.006
4. Dolomitic limestone, massive, biomicrosparite; many "eyes" of blocky calcite spar; bioturbated texture; fossils mainly sand sized, unidentifiable because of diagenesis	0.30
3. Shale parting, noncalcareous, grayish-brown, laminated, finely silty, discontinuous. Mainly illite with minor quartz and accessory illite/smectite and dolomite	0.012
2. Dolomitic limestone, massive, bioturbated texture throughout. Lower part micritic/microsparitic mudstone with sparse ostracode fragments; upper part biomicritic wackestone, fossils largely obliterated during diagenesis; calcispheres common; forams sparse	0.88
1. Limestone, micritic mudstone; scattered grains of quartz silt and very fine sand; locally brecciated and cemented by microsparite; top of bed uneven. Very bioturbated, *Chondrites* abundant, calcispheres locally common	0.46
Total thickness of measured section at Stop 6a .	8.75 m

*Section measured by D. E. Hattin in 1991.

DESCRIPTION OF MEASURED SECTION AT STOP 6c*
(Units 1-14 are described in the measured section for stop 6b, which follows)
(see figure 33)

St. Louis Limestone (part)	thickness (meters)
28. Limestone, not sampled (inaccessible)	0.61
27. Limestone, massive, biomicritic packstone with bioturbated texture. Brachiopod and echinoderm debris and forams abundant; ostracodes and bryozoan debris common; calcispheres and possible mollusc debris sparse	0.76
26. Limestone, massive, biomicritic wackestone/packstone, grains very poorly sorted; lower part contains sparse biomicritic wackestone-filled burrows; upper part with	

strongly preferred orientation of large grains parallel to stratification. Bryozoan, brachiopod, and echinoderm debris abundant; ostracodes and calcispheres common; gastropods sparse 1.19

25. Limestone, chert-bearing, basal part biomicritic packstone/biosparite with bioturbated texture and discrete biomicritic wackestone-filled burrows; grains poorly sorted, silt to granule sized. Middle and upper parts predominantly massive biomicritic wackestone, with bioturbated texture and some discrete micrite-filled burrows. Unit preserves overall fining-upward character; contains numerous thin to very thin chert beds and discontinuous layers of chert nodules. Brachiopod, bryozoan, echinoderm, and indeterminate skeletal debris abundant; ostracodes and calcispheres common; forams sparse 2.29
24. Shale parting, medium-yellowish-gray, calcareous, slightly silty 0.015
23. Chert, texture and fossil content as in unit 22, rock largely replaced by microcrystalline quartz. Crinoid columnals and fenestellid bryozoans abundant 0.024
22. Limestone, earthy, cherty, biomicritic packstone/biosparite, local patches of biomicritic wackestone as burrow filling. Crinoid, brachiopod, bryozoan, and indeterminate skeletal debris abundant; well-preserved productoid brachiopods and fenestellid bryozoans abundant; ostracodes, calcispheres, and burrow structures common. Part of rock and some isolated skeletal grains replaced by microcrystalline quartz (=chert) 0.076
21. Shale parting, medium-yellowish-orange, calcareous, slightly silty 0.015
20. Dolomitic limestone and silicified limestone, massive, originally a biomicritic packstone with silt- to fine-pebble-sized grains; matrix in part recrystallized to coarsely crystalline dolomite; much of rock has matrix recrystallized to finely crystalline silica (=chert). Echinoderm, bryozoan, and brachiopod debris abundant; forams, calcispheres, and ostracodes common ... 0.1
19. Shale parting, dusky yellow-green, noncalcareous, silty; very thin small lenses of earthy crinoidal limestone, partly replaced by chert 0.006-0.009
18. Calcitic dolostone, massive microcrystalline "mudstone," sparse burrow structures; very sparse grains of quartz silt and very fine sand 0.29
17. Shale parting, dusky-yellow-green, noncalcareous, silty. Very thin local lens of pelletiferous biomicritic packstone/biosparite; bryozoan, brachiopod, and echinoderm debris abundant; ostracodes and calcispheres common 0.009-0.012
16. Limestone, massive, biomicritic packstone, local patches of biomicritic wackestone and biosparite, bioturbated texture throughout; grains range from silt to coarse-sand size. Echinoderm, brachiopod, bryozoan, indeterminate skeletal debris and forams abundant; ostracodes common; calcispheres sparse; silicified *Acrocyathus proliferus* colonies common in two intervals; top of bed marked by concentration of orthotetid and spiriferid brachiopods. Unit brecciated in local collapse feature adjacent to measured sections 0.98
15. Calcitic dolostone, massive, microcrystalline "mudstone"; dolomite-filled voids and fractures and widely scattered grains of quartz silt and very fine sand; dolomite crystal size increases upward; quartz content decreases upward; recrystallized crinoid debris very sparse. Small tabular chert nodules 0.15 m above base. Unit extends downward into collapse feature adjacent to measured section 1.22

Total thickness of measured section at Stop 6c ... 7.58 m

*Section measured by D. E. Hattin in 1991.

DESCRIPTION OF MEASURED SECTION AT STOP 6b*
(see figure 33)

thickness (meters)

St. Louis Limestone (part)

14. Calcitic dolostone and dolomitic limestone; basal 0.3 m massive, micritic to microsparitic mudstone with sparse grains of quartz silt to very fine sand, riddled by *Chondrites* that are filled with micrite; *Chondrites* present in diminishing numbers to about 0.21 m above base; upper half of unit massive micritic wackestone to microcrystalline "wackestone" with much dolorhombic texture, bioturbated. Recrystallized skeletal debris common throughout, echinoderm and brachiopod remains barely identifiable; grains of quartz silt and very fine sand scattered throughout. At Stop 6c this unit is merged with unit 15 ..... 0.69
13. Calcitic dolostone; basal 0.17 m with undulatory, alternately tightly cemented ledge-forming layers and less well cemented recessed layers; mostly microcrystalline, alternating coarser and finer grained irregular laminae; sand-sized intraclasts sparse; calcite- or dolomite-filled millimeter-scale burrows common, some burrows lined with micrite; scattered grains of silt- to fine-sand-sized quartz. Upper part of unit not well laminated, contains micrite-filled centimeter-scale burrows or desiccation cracks filled with micritic mudstone containing spar-filled millimeter-scale burrows 0.27

———DISCONFORMITY———

12. Shale parting, grayish-olive-green, noncalcareous, silty, discontinuous 0.003-0.015
11a. Calcitic dolostone, microcrystalline, widely scattered grains of silt- to medium-sand-sized quartz; micritic intraclasts and possible pellets common; microstylolites common; contains micritic fragments of possible algal structures. This rock occurs in

narrow, downward-tapering wedges that are sharply truncated by overlying stromatolitic bed (unit 13). Some wedges extend as far as unit 5. Similar rock occupies depressions at top of adjacent breccia-filled sinkholes .....

11. Limestone, massive, thoroughly bioturbated, patchily distributed micritic mudstone, biomicritic wackestone/packstone, and small amounts of biopelsparite; scattered grains of quartz silt. Echinoderm and brachiopod debris abundant; forams and ostracodes common; bryozoan debris and calcispheres sparse. Unit pinches and swells laterally; fractured, fractures filled with very finely crystalline gypsum 0.26
10. Shaly limestone parting, greenish-gray, discontinuous, in places predominantly greenish-gray noncalcareous shale. Forms reentrant 0.006
9. Limestone, massive, biomicritic wackestone with local patches of pelsparite, bioturbated; numerous discrete burrow structures; silt-sized quartz grains sparse; unit pinches and swells laterally. Ostracodes common; echinoderm and mollusc or brachiopod debris, forams, and calcispheres sparse 0.23
8. Shaly limestone parting, greenish-gray, pinches out laterally. Forms reentrant 0.02
7. Limestone, massive, thoroughly bioturbated, with patchily distributed fossiliferous micrite, biomicritic to pelmicritic wackestone/packstone and very small amounts of biosparite/pelsparite; irregular ovoid areas of blocky calcite suggest birdseye structure; unit thickens laterally to as much as 0.52 m. Forams and ostracodes common; bryozoan debris and gastropods sparse; millimeter-scale bushlike algal structures common 0.30
6. Shaly limestone, dark-olive-gray, discontinuous, intramicritic/biomicritic wackestone grading upward to solution-packed packstone with horsetail structure. Crinoid debris common to abundant; brachiopod fragments common. Forms noticeable reentrant 0.07
5. Calcitic dolostone, massive, micritic mudstone with laminated interval 0.20 to 0.34 m above base; laminated interval in part cross-laminated, locally contains intraformational conglomerate; quartz silt common to abundant in alternate laminae. Burrow structures common locally; molds of brachiopods and crinoid columnals sparse. Topmost 0.08 m tightly cemented, highly fractured "crust" consisting, from bottom to top, of micritic mudstone that contains large dolomite-filled fractures, brecciated micritic mudstone cemented by microcrystalline dolomite and containing fewer dolomite-filled fractures, and brecciated microcrystalline dolostone cemented by coarser grained microcrystalline dolostone and by finer grained microcrystalline dolostone in which ghosts of breccia clasts are visible. Dolostone-filled fractures described under unit 11a reach their downward terminations in upper part of unit 1.22
4. Silty dolomitic limestone with crystalline poikilotopic texture; abundant uniformly distributed quartz silt and very fine sand. Discontinuous 0.05
3. Shale parting, noncalcareous, dark-greenish-gray, silty 0.003
2. Calcitic dolostone, micritic mudstone containing scattered grains of quartz silt, in part brecciated; matrix of brecciated part is micrite/microsparite containing abundant grains of quartz silt and very fine sand and a few grains of mica and heavy minerals 0.09
1. Silty dolomitic limestone with crystalline poikilotopic texture; abundant grains of quartz silt and very fine sand; mica and heavy minerals sparse 0.11

Total thickness of measured section at Stop 6b ..... 3.32 m

*Section measured by D. E. Hattin and S. H. Swain in 1990 and 1991.

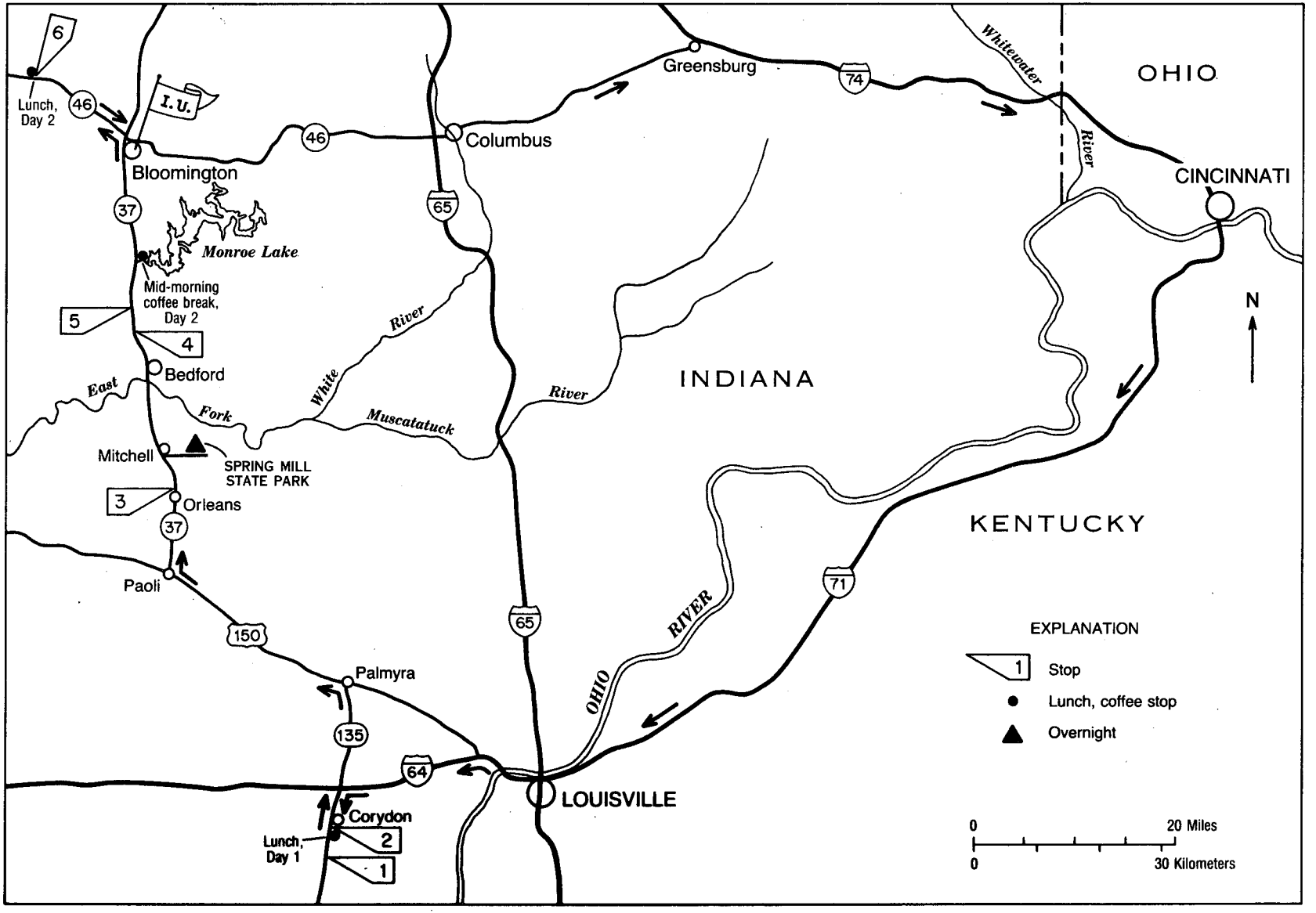

MAP OF FIELD-TRIP ROUTE.